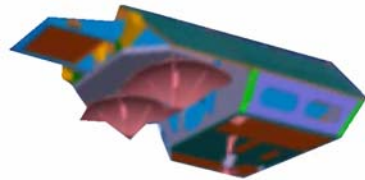


Airborne ice altimetry methods for calibration and validation of CryoSat results

PhD Thesis

Sine Munk Hvidegaard



Niels Bohr Institute, University of Copenhagen
and Danish National Space Center
July 2005

Advisors:

Prof. C. C. Tscherning, University of Copenhagen
State Geodesist R. Forsberg, Danish National Space Center

Preface

The work reported here is part of the Cryo-DK project funded by the Danish Research Council. This thesis is submitted to the Faculty of Science, University of Copenhagen in July 2005 for evaluation for the PhD degree. The submitted material consists of the thesis following next and 3 appended papers and 2 reports listed below. Copies of the papers are found in the back and the reports are attached separately along with author statements addressing the specific contributions.

Appended material:

- [1] **Hvidegaard, S. M.** and R. Forsberg: Sea-Ice Thickness from Airborne Laser Altimetry over the Arctic Ocean North of Greenland, *Geophys. Res. Lett.*, 29(20), 1952, 2002.
- [2] Forsberg, R., K. Keller, **S. M. Hvidegaard** and A. V. Olesen: ESAG-2002, European gravity and lidar survey in the Arctic Ocean, *KMS Technical Report*, NO. 21, 2003.
- [3] Keller, K., **S. M. Hvidegaard**, R. Forsberg, N. S. Dalå, H. Skourup and L. Stenseng: Airborne lidar and radar measurements over sea-ice and inland ice for CryoSat validation: CRYOVEX-2003 final report. *KMS Technical Report*, NO. 25, 58p, 2004.
- [4] Giles, K. A. and **S. M. Hvidegaard**: Comparison of space borne radar altimetry and airborne laser altimetry over sea ice in the Fram Strait, *Int. J. of Remote Sensing*, in press, 2005.
- [5] **Hvidegaard, S. M.**, R. Forsberg, C. Haas, and A. Pfaffling: Comparison of sea-ice thickness measured by laser scanning and electromagnetic methods in preparation for ESA's CryoSat mission, submitted to *Int. J. of Remote Sensing*, 2005.

Abstract

European Space Agency's first Earth Explorer Mission, CryoSat, is planned for launch in September 2005. The goal of CryoSat is to monitor elevation changes of the Earth's cryosphere using an advanced radar altimeter. To be scientifically useful the results of CryoSat must be geophysically calibrated and validated. This will be done by the European Space Agency, ESA, in cooperation with international partners. The presented work is carried out in support of CryoSat. Methods for validation of the satellite mission results are evaluated by experimental work and data analysis. Data have been gathered using the Danish National Space Center airborne laser altimetry system. Extensive data processing and comparative analysis have been performed taking different sources of sea ice and land ice information into consideration. Results show that validation activities may be carried out using a combination of ground and airborne surveys to bridge from local in situ measurements to larger scale satellite sampling. Especially the combination of laser and radar altimetry operated from the same airborne platform shows promising results both over ice and snow covered land and ocean. Over sea ice, additional measurements with helicopter-borne electromagnetic techniques provide useful independent observations.

Resume

Det Europæiske Rumfarts Agentur, ESA's første Earth Explorer Mission CryoSat er planlagt til opsendelse i september 2005. CryoSats formål er at observere cryosfærens højdeændringer ved brug af et avanceret radaraltimeter. For at have videnskabelig værdi er det nødvendigt at foretage geofysisk kalibrering og validering af CryoSats resultater. Dette vil blive udført af ESA i samarbejde med internationale partnere. De præsenterede undersøgelser er udført for at underbygge CryoSat missionen. Udfra eksperimentelle undersøgelser og dataanalyser er metoder til validering af satellit missionens resultater evalueret. Data til dette er blevet indsamlet ved hjælp af Danmarks Rumcenters flybårne laseraltimetersystem. Omfattende databehandling og sammenlignende analyser er foretaget, hvor forskellige informationer om havis og landis er inddraget.

Resultaterne viser at validerings aktiviteter kan udføres med en kombination af overflade- og luftbårne opmålinger. Denne kombination kan danne bro mellem lokale in situ målinger og satellitobservationer på større skala. Specielt kombinationen af laser- og radaraltimetri opereret udfra samme luftbårne platform viser lovende resultater både over is- og snedækket land og hav. Over havis vil observationer fra helikopterbåren elektromagnetisk teknik give nyttige uafhængige informationer.

Acknowledgements

The research presented in this thesis is a result of interactions and cooperation with many persons under different projects and I would like to express my gratitude to everybody who contributed.

Special thanks to:

- My advisors Prof. C. C. Tscherning and State Geodesist R. Forsberg for encouragement and valuable advice.
- The European Space Agency and the EU fifth framework projects SITHOS and GreenICE for co-funding different field campaigns.
- The Swedish icebreaker Oden's crew for hosting our camera during the 2002 cruise.
- The Centre for Polar Observation and Modelling, University College London, especially Prof. D. Wingham, Dr. S. Laxon and K. Giles, for making a fruitful and pleasant visit possible.
- My colleagues, present and former, for their very extensive work during field campaigns and with data processing; and also for good discussions and friendship.
- Eva for many good PhD-student talks
- To my dear friends and family for being there during fieldwork and the last period of hard work.
- For good suggestions from those who helped improve this thesis.

Finally, and most important, I would like to thank Peter and Sofie for moral and practical support and for their patience during field campaigns, traveling, and the last time of writing this thesis.

Table of contents

1	Introduction	7
2	The CryoSat Mission	10
2.1	Mission facts	11
2.2	Instruments on board.....	12
2.3	Measurement principle.....	14
2.4	Calibration and Validation	17
3	Experiments	20
3.1	Aims of Cryo-DK	20
3.2	Field Campaigns	21
3.3	Technical Description	23
3.4	Standard Data Processing	27
4	Studies of sea ice	33
4.1	Procedure for determining freeboard	34
4.2	Estimation of sea ice thickness	38
4.3	Ice thickness maps	39
4.4	Comparison to other types of data	43
4.4.1	HEM-system and related ground surveying	44
4.4.2	Oden webcam.....	48
4.4.3	Radar versus laser incl. D2P	51
4.5	Summary of sea ice results	56
5	Studies of land ice	58
5.1	Repeated observations	59
5.2	Laser versus radar	61
5.3	Summary of land ice results.....	63
6	Conclusions	64
	BIBLIOGRAPHY	
	ACRONYMS	
	APPENDED MATERIAL	

1 Introduction

The cryosphere consists of the Earth's snow- and ice-covered areas. It plays a central role in the global radiation budget and is also the largest potential source of sea level fluctuations. Changes in the cryosphere's ice masses are not accurately enough known for climate change studies and are therefore essential to quantify and understand. At present time, it is unsure whether any reported change is due to global warming, inadequate observation techniques, or due to natural variability.

One part of the cryosphere is the ice on polar oceans, the sea ice. Melt of sea ice will not change the sea level but is particularly important for the heat exchange between ocean and atmosphere. Existing global ocean-atmosphere climate models are yet too simplified to reproduce observed sea ice extent. New models are being developed and need verification, especially observations of sea ice thickness. This is important in order to determine the accuracy of heat fluxes between the atmosphere and the ocean. For global monitoring satellite methods are most efficient but for sea ice thickness measurements satellite radar altimetry has only recently proved useful (Laxon, 2003). Ice elevation relative to the ocean surface, the freeboard, is observed by differing between echoes from ice and ocean. From freeboard measurements the sea ice thickness is estimated using an assumption of isostatic balance between the weight of the ice and the seawater surrounding the ice, together with ice and snow properties from climatology. From observations of ice thickness, the total mass of sea ice can be found from measurements of the ice extent. Satellite radar altimetry for sea ice observations have until recently been limited both by gross resolution and poor coverage of the Polar Regions.

The other important part of the cryosphere is ice masses on land in ice sheets and glaciers. Changes in the mass of ice will significantly affect the sea level and fresh water budget of the oceans. Elevation change observations are used to study the mass balance of ice sheets and glaciers on global scale. Elevation change measurements are also feasible by satellite altimetry. Until now the best results are from Envisat, ERS and Topex/Poseidon missions but only ice sheet interior have been monitored. The reason is that the altimeters have been designed for low-curvature surfaces like the ocean and therefore lose track of the signal over sloping terrain. This is a significant limitation since the largest changes are expected in margins, where slopes are greatest, caused by the largest exposure to forcing from ocean and atmosphere.

New satellite missions have been designed to improve monitoring of the cryosphere. The first satellite aimed at improving polar observations is the US National Space Agency, NASA, Ice Cloud and Elevation Satellite, ICESat, launched in January 2003. The primary instrument in ICESat is a laser altimeter used for mapping Earth elevations with a footprint of 60 m. The next satellite mission dedicated to cryospheric observations will be the European Space Agency's, ESA's, CryoSat due to launch in September 2005. It will carry a more advanced radar altimeter than the recent radar altimeter missions in order to provide higher resolution and better observations over sloping terrain.

The desire to gain more knowledge about these issues lead to defining the specific goal for the CryoSat mission. In short the primary mission goal is to determine trends in mass of the Earth's permanent ice fields. These goals will be meet by observing the following (ESA, 1999):

1. Regional and basin-scale trends in perennial Arctic sea ice thickness and mass
2. Regional and total contributions to global sea level of the Antarctic and Greenland ice sheets
3. Seasonal cycle and inter-annual variability of sea ice mass and thickness
4. Variation in thickness of the World's ice caps and glaciers

The first two are considered as primary goals and the last as secondary.

Point one will be observed through determination of sea ice thickness from elevation measurements. Combining this with ice extent from passive microwave radiometry will quantify total mass changes. The contribution of ice to the oceans will be assessed through mass balance studies using measured elevation changes of the ice sheets. Finally, point 3 and 4 will be addressed with monthly mapping of average elevations of inland ice and average thickness for sea ice covered oceans.

In the following, methods are examined for validation of the CryoSat results. Both experimental fieldwork and data analysis have been carried out and the results are not only valuable in connection to the satellite mission but carry weight themselves as contributions to a better understanding of the cryosphere.

Structure of the thesis

Chapter 2 gives a more detailed description of the CryoSat mission and the need for calibration and validation activities. In chapter 3 an overview of the fieldwork that has been used for the analysis presented in chapter 4 and 5. Chapter 4 deals with studies related to sea ice and chapter 5 outlines the work carried out in relation to inland ice. Finally in chapter 6 conclusions are given along with some recommendations for future research. In the end references and acronyms are listed.

2 The CryoSat Mission

CryoSat is the first of European Space Agency's Earth Explorer Opportunity Missions. It was proposed in 1998 by a team of scientific investigators lead by D. Wingham (Wingham et al. 1998) and is planned for launch in September 2005. The primary instrument of the payload is the SAR Interferometric Radar Altimeter, the SIRAL. The CryoSat mission has succeeded in being a low cost science driven satellite project, the first of the Earth Explorer Missions. It is dedicated to observations of elevation changes of the Earth's cryosphere. The aims are both inter-annual variations and trends in the mass of land ice and sea ice.

Requirement (cm/yr)	Arctic Sea Ice (area: 10^5 km^2)	Ice Sheet Interior ($14 \times 10^6 \text{ km}^2$)	Ice Sheet Margins (10^4 km^2)
σ_r	3.5	0.76	8.3
σ_m	1.6	0.17	3.3
Mode	SAR	LRM	SARin

Table 1.1. Science and measurement requirements of the CryoSat mission. The residual uncertainty of the measurement σ is defined for each zone of interest and the related SIRAL operating mode (ESA/UCL, 1999).

The measurement uncertainty requirements for each mode are given in table 1.1. The accuracy requirements for the mission are defined in order to be within 10 % of the uncertainties coming from natural variabilities at the end of the mission. In addition to this a higher spatial resolution compared to previous space borne radar altimeters is needed for mapping of sea ice and sloping parts of ice sheets and glaciers. Both of these requirements lead to the selection of the SIRAL instrument as the key instrument on CryoSat.

Microwave radar altimeters are routinely being used over oceans with an accuracy of a few centimetres (Fu and Cazenave, 2001) but they all have limited use over sloping terrain and sea ice. The new radar altimeter design with along track coherency and dual antennas for interferometry will significantly improvement observations of these targets. More details of the mission, payload and scientific goals are discussed below.

2.1 Mission facts

CryoSat started by a comparative call in 1998 and was approved by ESA in 1999. It has been designed, build and tested. The launch will take place from Plesetsk in Russia using a Russian launcher (ESA, 2001). The satellite is designed to have a 3-year lifetime and is hoped to last for up to 7-8 years. There will be a commissioning phase lasting 6 months after launch. Post launch tests and calibrations will take place along with initial data validation activities.

CryoSat will be placed in a non-sun-synchronous drifting low-Earth polar orbit. The mean altitude will be 717 km with an inclination of 92 degrees giving a 369 day repeat cycle with a 30 day pseudo sub-cycle. This is chosen as a trade-off between achieving good ground track coverage and high density of orbit cross over points. With this orbit selection CryoSat will reach polar areas up to 88 degrees (N/S) and cover for instance South Greenland with a track spacing of a few km.

The instrument payload is 720 kg including 36 kg of propellant (for orbit manoeuvres). The dimensions are 4.5 by 2.3 meters in length and width and the height is 2.2 meters. See Figure 1 for a view of the satellite. The power is generated by solar panels on two sides of the satellite and stored on Li-ion batteries.

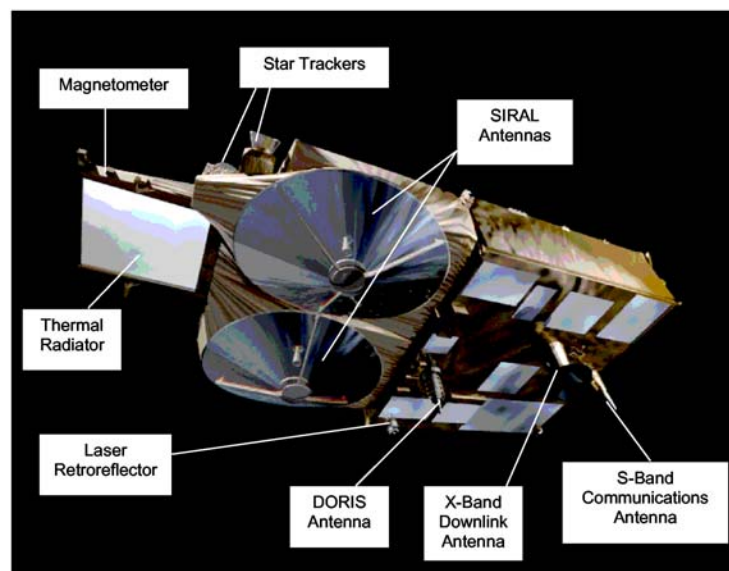


Figure 1. Illustration of CryoSat showing the instruments (Courtesy ESA).

The attitude and orbit is controlled by magnetotorquers and cold-gas micro-thrusters. Three star trackers and magnetometers provide precise information about attitude.

All data are stored on board in a solid-state recorder capable of handling 320 Gbits per day. Data will be down-linked through the X-band antenna via a single ground station in Kiruna, northern Sweden, at each pass over the station. Telecommunication to the satellite is done using an S-band antenna.

The most important mission facts are summarized in table 1.2.

CryoSat Mission Overview	
Launch	September 2005
Lifetime	3 years
Altitude	717 km
Orbit	LEO, non-sun-synchronous
Inclination	92 degrees
Repeat Cycle	369 days (30 day sub-cycle)
Dimensions	4.60X2.34X2.20 m
Mass	669 kg (incl. 336 kg fuel)
Communication	S-band
Data-link	X-band
Payload	SIRAL (primary)
	DORIS
	Laser Retro-reflectors
	Star Trackers

Table 1.2. Summary of CryoSat mission facts.

2.2 Instruments on board.

The payload of instruments onboard CryoSat were listed in table 1.2 and more details about the specific instruments are given below along with a short description of the ground segment.

SIRAL

As mentioned above the SIRAL, SAR Interferometric Radar ALtimeter, is the primary payload. It is build on a conventional pulse limited Ku-band radar altimeter, heritage of the Topex-Poseidon and Jason missions. Unique for the SIRAL instruments is that the along track resolution is enhanced by a high pulse repetition frequency, PRF, that allows coherent sampling and processing. Through the use of delay-Doppler algorithms, the effective along-track footprint will be an order of magnitude smaller than conventional radar altimeters (Raney, 1998). Also new is the possibility for across track interferometry provided by the two antennas and two receive chains. One antenna only receives and the other both transmits and receives. There are three operating modes that will be described later.

DORIS

The Doppler Orbit and Radio Positioning Integrated by Satellite, DORIS, is providing orbit positions for CryoSat. The system is also used for time reference signal for SIRAL and for ionosphere modelling. The time is referred to TAI, the international atomic time reference. DORIS is a radio frequency tracking system based on the Doppler principle and is supported by about 50 beacons on ground. On board the Doppler shift is measured every 10 seconds from the continuously transmitting beacons on two frequencies, 2036.25 MHz and 401.25 MHz. Observing on two frequencies makes it possible to model the dispersive ionosphere.

Star Trackers

A set of three star trackers is used to determine the orientation of SIRAL. This 3 axes attitude measurement is supported by high accuracy inertial attitude measurements. The star trackers are mounted on the space-exposed side of the antenna bench to ensure stability between the star sensors and the antenna frame.

LRR

Laser Retro-Reflector, LRR, is a passive optical device. It reflects ground-to-satellite laser distance observations and is therefore mounted on the Earth facing side of CryoSat to ensure good visibility. LRR is used to give an independent control of the precise orbit determination from DORIS.

Ground segment

The Ground Segment has 4 main functions:

1) Delivers output data.

The ground segment consists of both the receiving facilities in Kiruna and the data processing, archiving and distribution facilities. The data products are

- The Full-Bit-Rate product that consists of the instrument output data before averaging. The data are geolocated, dated and corrected for engineering and geophysical corrections.
- The level 1b product, the radar echoes that are averaged in the synthetic aperture modes (modes listed later) and three, the level 2 products.

- The level 2 products. These are the surface elevations along satellite orbits, which are averaged in space and time depending on target. Included are maps of sea ice thickness.

The first two are delivered within a few days of acquisition and the third depends on temporal averaging.

2) Mission planning.

3) Satellite command and control.

4) Calibration and delivery of near-real-time processed data products for validation purposes.

The above part is based on the Mission and Data Description Document, ESA (2001) and more details can be found there.

2.3 Measurement principle

The basic altimeter measurement is an observation of the travel time from instrument to the target and back. From this the distance, d , between the measurer and the target can be found as

$$d = \frac{ct}{2}$$

where t is the two way travel time and c is the signal velocity, for electromagnetic signals this is the speed of light. The conventional radar altimeter, that SIRAL is based on, operates after this principle.

To meet the requirements of observing sea ice freeboards and mapping sloping ice sheet margins, new more advanced techniques are used for the SIRAL design. The Ku-band microwave (2.2 cm wavelength) radar altimeter is pulse-limited and has a very high pulse-repetition-frequency, which gives along track coherent return signals that allows synthetic aperture processing. This mode of operation is illustrated in Figure 2.

By accounting for the Doppler shift from off nadir parts of the echo from each radar footprint, the footprint can be separated into several strips across track called Doppler beams. Each strip will be 250 meters wide along track and by superimposing strips from successive echoes, noise can be reduced by averaging. This mode is called the Synthetic Aperture Radar mode – the SAR mode.

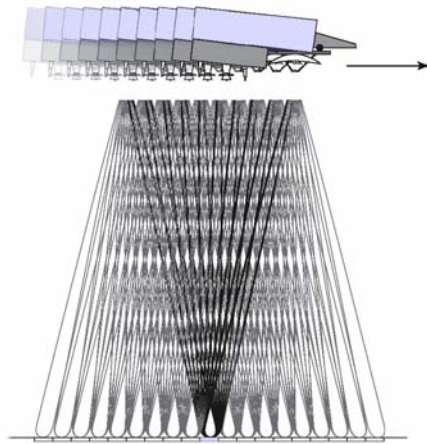


Figure 2. Illustration of the Doppler technique used for the synthetic aperture processing (ESA).

When receiving the echoes simultaneously on the second antenna the arrival angle can be determined. For an echo not directly nadir of the satellite the path length will be longer giving a small (up to the 2.2 cm wavelength of the radar signal) phase shift compared to a nadir target. Observing this phase shift between signals received by the two antennas provides the angle between the baseline, joining the two antennas, and the direction of the returned echo. This is only possible when the baseline is accurately known. This is illustrated in Figure 3 where the phase shift i.e. the path length difference is shown in red. For a target area with zero slope the phase shift will also be zero. This technique is known from interferometry and is therefore called SAR Interferometric mode or short, SARin mode.

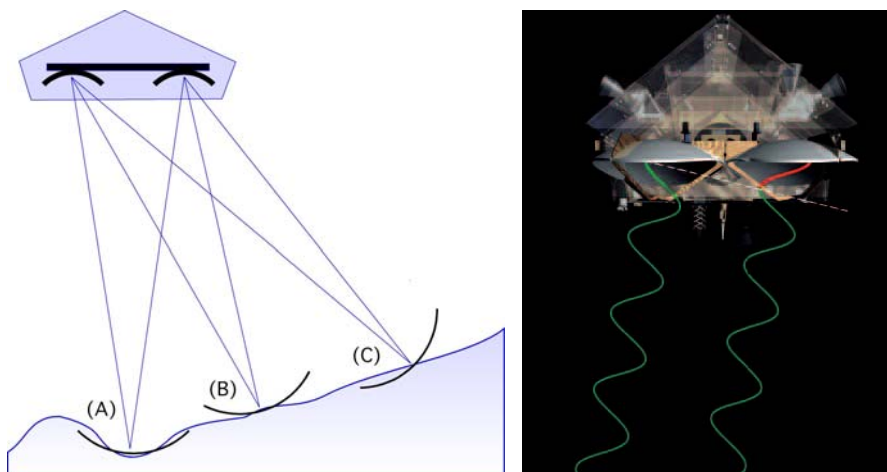


Figure 3. Illustration of SARin mode. Off nadir reflections will have different range between the surface and the two antennas shown as the red part of the signal on the figure seen to the right.

In summary this gives three operation modes:

- 1) LRM – conventional pulse limited mode operated over ice sheet interiors and oceans (not shown on the figure but recently it was decided to observe over oceans too).
- 2) SAR – Synthetic Aperture Radar mode is used for sea ice freeboard observations.
- 3) SARin – SAR mode with added interferometry using the dual antenna setup. This mode is used for marginal parts of ice sheets and over glaciers.

To limit the enormous amount of data generated by mode 2 and 3 a mask is used. An example of this is shown in Figure 4. This mask will vary throughout the year depending on the extension of the polar sea ice fields and is controlled by the ground segment.

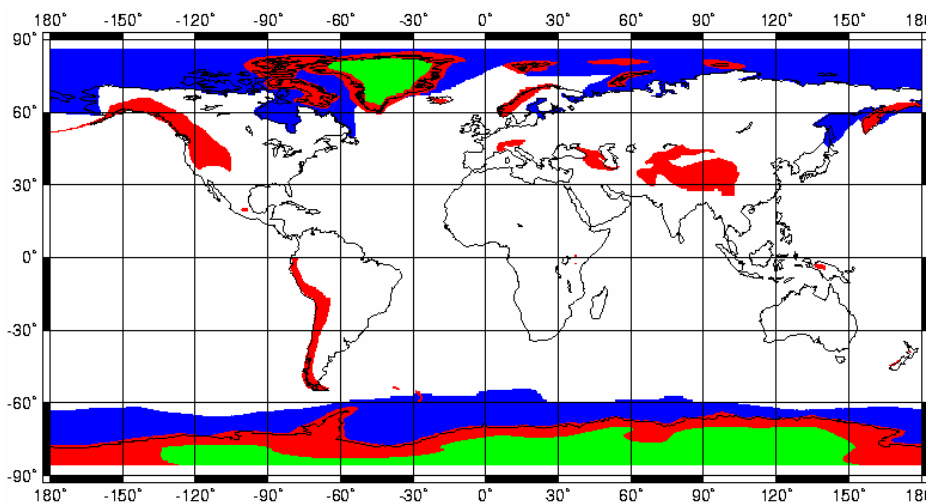


Figure 4. Example of the mask used for the different operation modes. Green: LRM, red: SARin mode and blue: SAR mode (ESA).

2.4 Calibration and Validation

In order to fulfil the goals laid out in the Introduction, chapter 1, with the accuracy presented in table 1.1 extensive calibration and validation of the SIRAL observations is needed. These activities are commonly known as cal/val activities. The overall purpose is to provide confidence in estimates of the uncertainty of CryoSat data products, and to understand the signals from glacial ice and sea ice especially concerning possible penetration effects (ESA, 2001). This is done as an iterative process starting from the launch of the satellite - even before launch some airborne Ku-band validation experiments has been performed. After the first cal/val attempts it will be possible to provide more insight into the product algorithms and open up for improvements. It is expected that reprocessing will be done later during the mission relying on this insight.

In general there are two contributions to the uncertainty of CryoSat's data products, (instrument-) system errors, ε_s , and retrieval errors, ε_r . The physical quantity measured is the echo i.e. echo-power, -delay-time, and -phase. The errors arise from the assumptions concerning the relation of thickness or elevation to the echo. The observation is retrieved by performing an operation L_r on the measured echo quantities. The total uncertainty can be expressed as

$$\varepsilon = \varepsilon_r + L_r \varepsilon_s$$

since the system error and the retrieval error can be assumed independent.

Level 1b data consist of the measured echoes, after Doppler processing, with ancillary measurements along the satellite. Level 1b data are obtained with errors ε_s . Level 2 data is the sequence of thickness or elevations along the satellite orbit associated with errors ε_r . (The level 1b processor converts the satellite telemetry to 1b data and the level 2 processor converts 1b data to 2). With this in mind, calibration can be seen as the estimation of the system errors and validation as the estimation of the retrieval errors. Summarized, "system errors arise from imperfect engineering and retrieval errors from an imperfect description of the scattering from the surface" (ESA, 2001 p. 8).

Independent calibration and validation is needed to maintain the independence between system errors and retrieval errors. Most of the calibration is done in advance of the launch but also in-orbit calibration is expected during the commissioning phase. The system errors are expected to give a small contribution to the total error budget. A larger contribution will come from retrieving errors and therefore a greater emphasis will be on the validation. A comprehensive evaluation of different uncertainties and suggested methods to estimate them is found in the CryoSat Calibration and Validation Concept document (UCL/ESA, 2001).

Plans for CryoSat calibration and validation activities were initiated by ESA's Announcement of Opportunity in November 2001. Interested parties could submit suggestions for methods and contributions to fieldwork aimed at the calibration and validation of CryoSat's products. A team of scientists were selected to form the Calibration and Validation Retrieval Team, CVRT. The purpose of the CVRT is to plan and perform the cal/val campaigns. This work is co-funded by ESA and CVRT members national funding. DNSC, represented by State Geodesist R. Forsberg, is one of the several international members of CVRT.

CVRT has outlined plans for cal/val activities and selected specific target areas, Figure 5. Both sites in Arctic and Antarctic regions are represented. For sea ice the areas are, the Arctic Ocean north of Greenland, Fram Strait between Svalbard and Northeast Greenland, and the Bay of Bothnia in the Arctic and the Weddell Sea in Antarctica. For land ice the chosen sites are the EGIG (Expédition Glaciologique au Groenland) line in Central Greenland, Devon Ice Cap in Canada, Austfonna Glacier in Svalbard, and Dronning Maud Land and the Antarctic Peninsula in Antarctica. The CVRT have also planned and carried out several pre-launch campaigns from 2002 to 2004. The scope of these was to test methods for validation and gather data for sites to be repeated for height change studies and assess the accuracy of the natural variability. Among these are the LaRA-2002 campaign, a laser and radar altimetry survey from a NASA P-3 aircraft (Raney and Leuschen, 2003), and the CRYOVEX-2003 campaign where laser and radar altimetry from a Twin-Otter aircraft were coordinated with ground and helicopter borne experiments based on the German research vessel Polarstern. Result from the CRYOVEX campaign along with other DNSC campaign results are discussed in coming chapters.

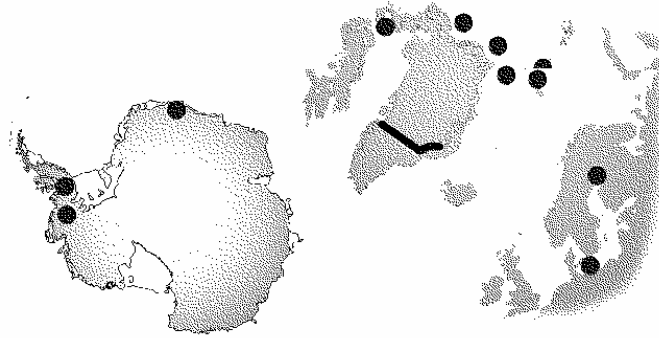


Figure 5. Calibration and validation sites chosen by the CVRT. Left: Sites in Antarctica. Right: Sites in Arctic and Scandinavia.(ESA)

For both inland ice and sea ice, timing and location of the validation campaigns must be carefully selected. Time variant errors can be assessed by repeated experiments. The preferred time period are the months of April and August/September to represent the maximum and minimum ice thickness and snow depth during the seasonal cycle. To bridge the spatial scales from local ground measurements to satellite data, coordinated ground and aircraft experiments are needed.

Some selected types of observations to be used for CryoSat product validation are:

For sea ice,

- In situ borehole ice thickness measurements and electromagnetic induction observations (both ground and helicopter borne)
- Airborne laser and radar altimetry coordinated with the above and also coordinated to under-fly actual CryoSat orbits

For land ice,

- In situ pit-studies, coring, and other probing in shallow drill-holes
- Transponder measurements to assess penetration issues (possibly also used in sea ice)
- Airborne laser and radar altimetry
- Modelling and assemble accumulation and ablation records

Comparisons to NASA's ICESat mission laser altimetry results will also be very valuable.

A special CryoSat type radar altimeter has been designed for the validation activities, the ASIRAS. ASIRAS will be operated both from a Dornier aircraft by the Alfred Wegener Institute, Germany, and the Twin-Otter with the DNSC laser scanner system. The plans for the CryoSat cal/val activities are being re-scheduled after the launch delay and the final plan will be ready after launch.

3 Experiments

In order to prepare for CryoSat final cal/val several initiatives were taken. Both analysis of existing data sets and new field activities were started to gather more information about the expected radar observations and about the natural variabilities of the land and sea ice targets for observations by CryoSat. One of these initiatives is the research project, “Cryo-DK”, funded by the Danish National Science Research Council under which this present study is a substantial part.

3.1 Aims of Cryo-DK

The goals of the project are to

- 1) Carry out field campaigns with airborne laser and radar altimetry, both to gather independent data sets describing the ice field and to prepare for actual satellite cal/val campaigns
- 2) To perform radar data processing similar to expected CryoSat data analysis.

Since the time of application ESA has decided to have the CryoSat data processing extended to level 2 (the original plan was only to deliver level 1b to the users). This processing will be done on behalf of ESA in cooperation with University College London, UCL, in UK. The level 1b processing, therefore has been toned down in the PhD studies under this research grant. The focus will be on pre-launch field campaigns in support of CryoSat cal/val plans, especially the CRYOVEX 2003 campaign.

During the field activities, airborne data from laser and radar altimetry has been gathered over both Arctic sea ice and Greenland inland ice. To the degree possible the campaigns have been designed to take advantage of other types of sea ice observations. This provides the opportunity to compare the airborne measurements to independent coincident and contemporaneous observations of the ice fields observed. In the following a short description of the field campaigns is given from which data have been analysed. All campaigns have been coordinated by R. Forsberg and carried out by the research group from the Geodynamics Department, DNSC (former Geodyn. Dept. National Survey and Cadastre, KMS) in cooperation with many international partners. Processing of the data sets have been a team effort of the Geodynamics Department over many years.

3.2 Field Campaigns

From the year 1996 DNSC/KMS has developed an airborne gravity system, and this has been used extensively since to map the gravity field in various countries starting with Skagerrak and the Azores in 1996-7 in the EU project AGMASCO (Airborne Geoid Mapping System for Coastal Oceanography). With US, Norwegian, and Danish funding, continental shelf regions surrounding Greenland and Svalbard were surveyed in 1998-2002 (Olesen, 2003). Major survey projects 2003-2005 include Malaysia and Mongolia. As a part of the technical setup for these observations, a near-infrared laser altimeter was used for altitude control. After the first field campaigns it became clear that these observations provided excellent data over sea ice and had potential to map the sea ice thickness (Hvidegaard and Forsberg, 2002). Besides that, the altimetry has been used to map the topography of inland ice. In 2001 the airborne system was extended with a scanning laser altimeter. This near-infrared laser instrument maps swaths of the surface providing more information about the surface characteristics. The width of the swaths is approximately the same as the flight-altitude.

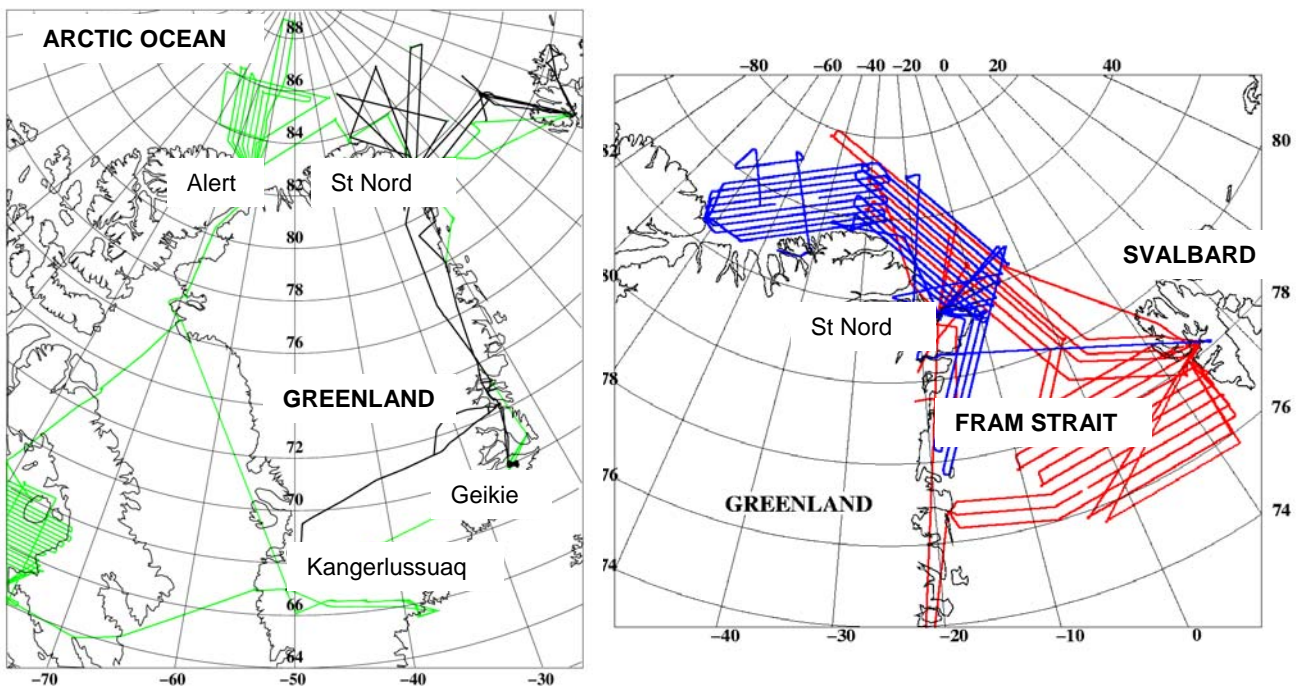


Figure 6. Flight tracks for all 4 years of Arctic ice surveys. Black: 2003, green: 2002, red: 2001 and blue: 1998.

Archived data from previous gravity campaigns as well as new data sets from 2002-3 campaigns specifically designed to observe ice covered surfaces has been used for the studies presented in the following chapters. A short description of the different campaigns is found below, listed by the year of measurements. Plots of the flight tracks can be found in Figure 6. The surveys have been documented in the KMS (now DNSC) Technical Report series where more details of the contents of the fieldwork and details of the data sets can be found (see references added below).

Archived data sets:

- 1998 Airborne gravity survey of the Arctic Ocean continental shelf. Single beam laser profiles were sampled for accuracy control of the GPS height determination. Survey flights were concentrated in the Arctic Ocean north of Greenland and near the North Greenland coast. (Forsberg et al., 1999)
- 2001 Airborne gravity survey. Single beam laser profiles and some laser scanner swaths were gathered near Northeast Greenland and in the Fram Strait. (Forsberg et al., 2002)

In 1999 and 2000 continental shelf area around Greenland were surveyed with the airborne gravity system. Only a very small part of these flight lines were over ice and none of these data have been used in the investigations presented here.

Data sets from sea ice and inland ice surveys:

- 2002 ESAG-2002. Joint laser scanner and airborne gravity survey north of Greenland and on marginal part of Greenland's ice sheet, partly sponsored by ESA. The goals were to fill out a void in the gravity coverage in the Arctic Ocean and sample different sea ice regimes. (Forsberg et al., 2003)

2003 CRYOVEX-2003. CryoSat Validation Experiment was co-funded by ESA and the European Union fifth framework projects SITHOS and GreenICE. The survey was used as a proof-of-concept for upcoming validation campaigns. Airborne laser scanner and CryoSat type, the D2P, radar altimeter was used for observations both over inland ice and sea ice. The survey was coordinated with measurements from the German research vessel Polarstern that based a helicopter with an electromagnetic induction sensor, HEM, for sea ice thickness measurements. (Keller et al., 2004)

This type of fieldwork has been continued in 2004 and latest in May 2005. The 2004 GreenICE campaign included both airborne surveying over the Greenland Ice Sheet and Arctic sea ice and an ice camp at 85N and 65W (Dalå et al., 2005). The 2005 campaign aimed at improving the method of gaining coincident airborne laser scanner and HEM observations, a last preparation for CryoSat validation, and repeating previously sampled areas in the Arctic Ocean north of Greenland (Hvidegaard and Olesen, 2005). Currently both data sets are being analysed.

3.3 Technical Description

A chartered Twin-Otter from Air Greenland a/s, the OY-POF see photograph Figure 7, was used for all surveys. This type of aircraft is well suited for operations in the Arctic because of the ability to land and take off from short unprepared airstrips. In addition to that, this particular airplane has a hole in the aft luggage compartment where the laser instruments can be mounted with direct view to the surface below. The availability of an autopilot for exact matching of planned flight lines is also very useful. The Twin-Otter was equipped with skis for most of the surveys. This gives an extra option to land on snow covered smooth surfaces for instance the Greenland ice sheet (as was done in 2002, for making snow pit studies) or directly on the sea ice (as for the 2004 GreenICE camp).



Figure 7. Photograph of the Air Greenland Twin-Otter (registration OY-POF) at Station Nord, Greenland 2003.

The basics of the instrumentation mounted in the Twin-Otter is:

- Laser scanner/single beam altimeter for range measurements between the aircraft and the surface.
- GPS antennas and receivers in order to position the aircraft i.e. the instruments.
- Inertial navigation unit that measures the accelerations and rotations of the aircraft in three dimensions to give angles of aircraft movements.
- Visual documentation by video cameras, digital cameras or web-cameras.
- Power conditioner and battery backup that converts aircraft power, 28 V, to 12, 24 and 230 V.
- Computers for data storage and instrument control.

More details of the instruments are found in table 2.1 and the standard setup in the aircraft is sketched in Figure 9. Photographs of the installation from 2002 are seen in Figure 8.



Figure 8. Photographs of the installation. Left: Rack with power conditioner, laptops, and GPS receivers. Right: Laser scanner

Altimeter	Single Beam Laser	Laser Scanner	
Type	ADM GPA 100	LMS-Q140i-60	
Manufacturer	Optech	Riegl	
Range (20% reflectivity)	0.2-350 m	300 m, scan angle 60 deg.	
Accuracy	5-10 cm	2.5-5 cm	
Wavelength	904 nm	900 nm	
Resolution	10 cm	2.5-5 cm	
Beam Divergence at 300 m altitude (footprint size)	0.3 deg. (1.6 m)	0.17 deg. (0.9 m)	
Measurement Rate	1-100 Hz	0-9900 Hz	
Inertial Navigation System		IMU	EGI
Type	Custom made	H764G	
Manufacturer	Greenwood Eng.	Honeywell	
Accuracy (pitch/roll)	0.1/0.5 degrees	0.05/0.05 degrees	
Measurement Rate	18 Hz	50 Hz	
Accelerometers	3 Schaewitz	3 QA-200	
Gyros	3 fibre-optics	3 laser gyros	
Geodetic GPS receivers	Trimble	Ashtech	Javad
Type	4000 SSI	Z-Surveyor Z-Extreme	Legacy
Measurement Rate	1 Hz	1 Hz	1 Hz
No. of channels	9	12	12
PPS option *	Yes	No	Yes

*For timing of other instruments

Table 2.1. Technical specifications of DNSC system instruments.

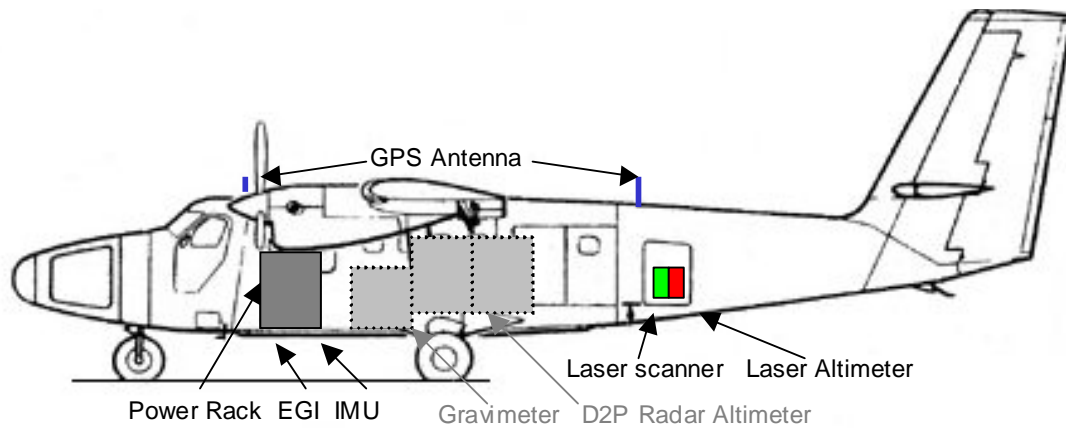


Figure 9. Sketch of how the instruments are mounted.

The instrumentation and technical setup has evolved over the years. The DNSC (former KMS) aerogravity system was used in the Arctic for the first time in 1998 (Olesen, 2003). Then it consisted of the Lacoste-Romberg gravimeter, a power conditioner, two GPS receivers, a prototype inertial measurement unit (the Greenwood IMU) and an Optech single beam laser profiler/altimeter (technical specifications in table 2.1). Since then survey hardware upgrades have been made almost every year. The power conditioner has been redesigned more than once, an additional GPS added (now two antennas and three different types of receivers), a better inertial navigation system, the Honeywell H7646 EGI was added in 2000, and the Riegl laser scanner (lidar) that was used for the first time in 2001. The laser scanner provides the opportunity to sample swaths of the surface below the instrument in addition to the along track observations by the single beam laser altimeter. The measurement principle of the laser scanner is shown in Figure 10.

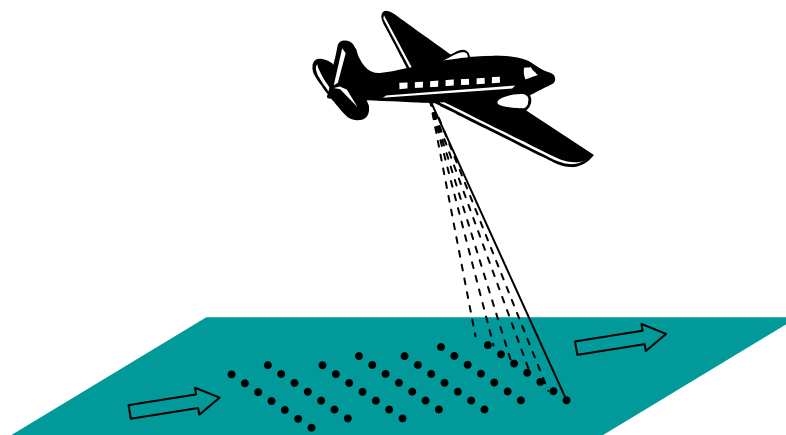


Figure 10. Laser scanner principle.

In 2003 the Johns Hopkins University/Applied Physics Laboratory, JHU/APL, Doppler Delay Radar Altimeter, D2P, (Raney 1998), was used along with the DNSC system from the Twin-Otter. The D2P is a 13.9 GHz radar operating from the same principle as the SIRAL onboard CryoSat. Instrument racks were mounted in the cabin and the radar antenna was mounted near the laser scanner under the aircraft, see photographs.



Figure 11. Photographs of D2P system. The antenna is seen to the left and the racks with the radar and data storages system from the cabin of the Twin-Otter is seen to the right.

3.4 Standard Data Processing

The principal method of observing the surface with laser altimetry from an airborne platform is displayed in Figure 12. The airborne platform, the aircraft, is positioned using the GPS system and the platform attitude changes are determined from an inertial navigation system (INS). The laser altimeter measures the range between the platform and the surface. By combining this range measurement with the knowledge about the platform attitude and position, the range can be converted into latitude, longitude and height of the surface target.

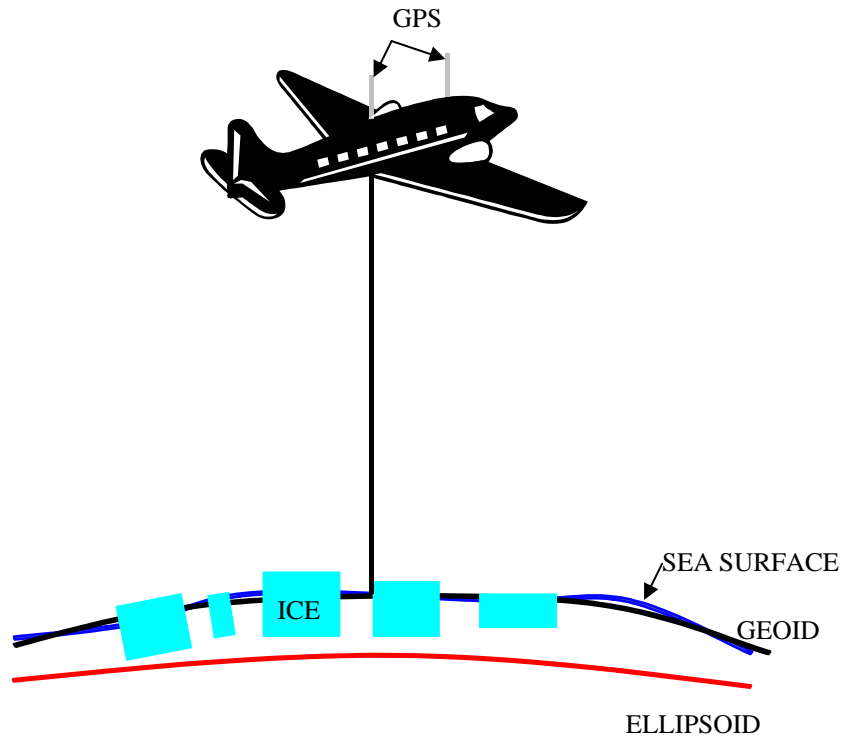


Figure 12. Airborne laser altimeter measurement principle.

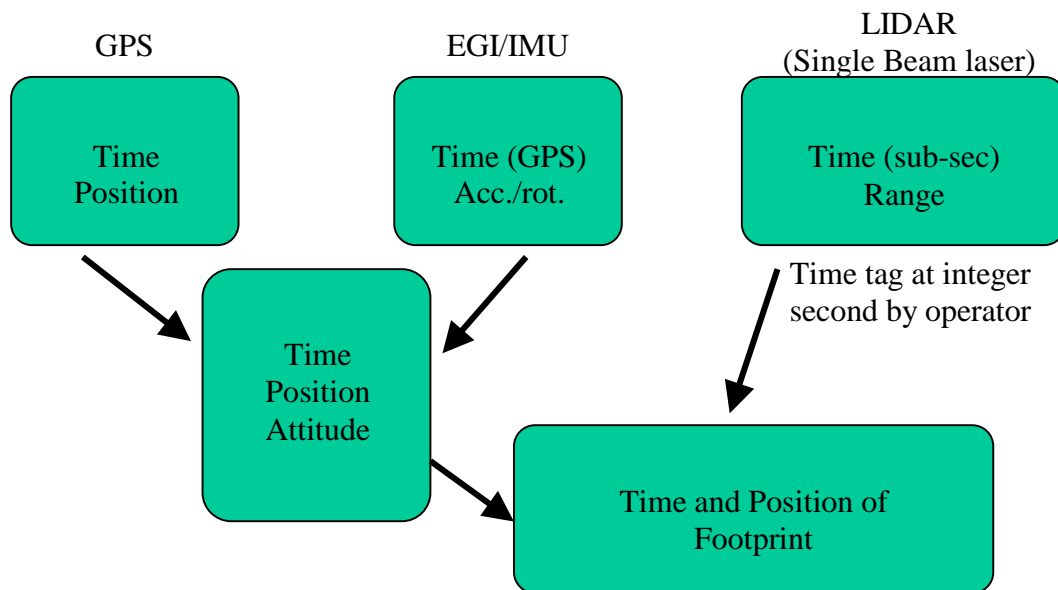


Figure 13. Flow diagram of the data processing.

In the following an overview of the data processing steps is given. The details are described in technical reports referred to in section 2.2. The principle of data analysis is outlined in the flow diagram in Figure 13. The differential kinematic GPS solutions are post-processed relative to reference ground stations (see photographs below) with precise International GPS Service, IGS, ephemeris. The accuracy of the GPS solution

depends on the distance from the reference station. Close to the reference, accuracies better than 10 cm can be obtained. For longer baselines, up to several hundred kilometres, only an accuracy of a few decimetres is possible. These are combined with acceleration and rotation information from the INS accelerometers and gyros to give position and attitude data. The advantage of the combination is that INS provides high-resolution measurements of the platform movements but suffers from drift problems and the GPS is more stable and can then constrain the output. This gives a stable positioning for the full flight time, 5-6 hours typically.



Figure 14. Photographs of reference GPS stations. Left: Antenna on top of building at Station Nord and right: Antenna on Danish Meteorological Institute's hut in Kangerlussuaq.

The position and attitude output is used to transform the laser range data from the local coordinate system in the aircraft to three-dimensional surface observations in a general reference system. The exact transformation formulas are for instance described in Andersen et al. (2005).

The IGS reference frame with different epochs is used. All data is time tagged using GPS time stamps.

Table 2.2 lists the data processing software used. The codes are written in FORTRAN by R. Forsberg and developed over the years by the users in the Geodynamics Department, DNSC. Figure 15 shows an example of sea ice mapping with the laser scanner along with photographs of the same section.

Single Beam Laser	Laser scanner	Comment
READINS	READEGI	Reads raw inertial navigation data files and reformats data
GPSINS	GPSEGI	Merges INS with GPS solution to provide position and attitude
READLAS*	READSCAN	Uses position and attitude information to transform range measurement to geolocated height

* Can also be used with GPSEGI output data and READSCAN can be used with GPSINS data if lack of EGI occurs.

Table 2.2. Overview of laser altimeter processing software developed for the DNSC airborne system.

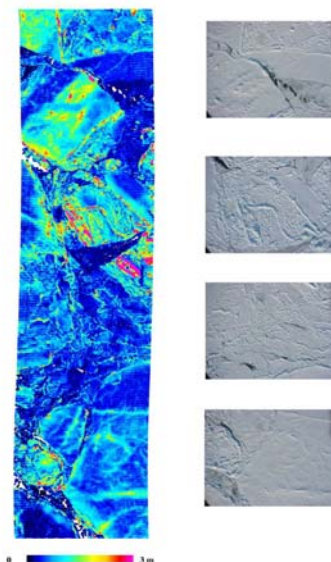


Figure 15. Examples of output sea ice elevation data from the laser scanner (2003 CRYOVEX survey). To the left is shown photographs from the nadir looking camera that was mounted next to the laser scanner.

The laser and INS instruments are rigidly mounted to the aircraft floor but it is impossible to avoid a small misalignment between the laser fixed coordinate system and the INS fixed system. These misalignment angles, called boresight angles, are constant throughout a survey. The typical procedure to determine these angles is to fly over GPS-positioned objects for instance a building. The optimal way is to fly a four-leaf clover path in order to get control over all directions.

Data from such a calibration flight is seen in Figure 16. The boresight angles are typical less than one degree.

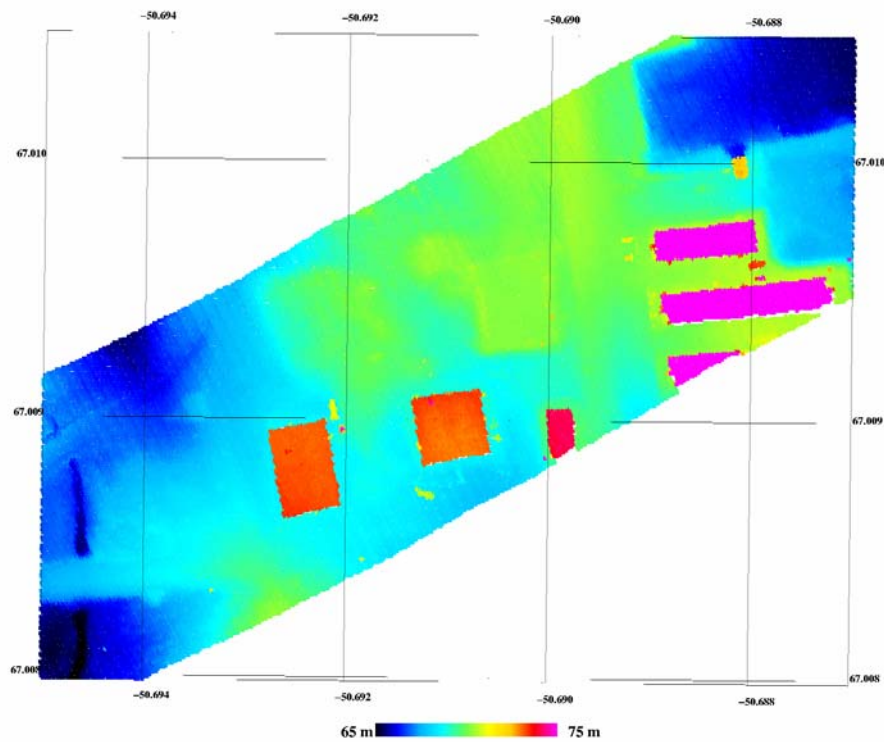


Figure 16. Example of data from calibration flight over building in Kangerlussuaq, Greenland.

Flight lines over known targets, such as a building or a runway or a cross-over of tracks, can also be used for data quality control purposes. This type of system validation was done in connection with a small survey in Denmark. Here a road (on a dam to Rømø) was surveyed with GPS from a car and the same road was measured by the laser scanner-GPS-EGI system operated from a Piper Navajo PA 31 airplane. Comparing the data sets gave an excellent fit: the mean difference was found to be 2 cm with a standard deviation of 8 cm (Andersen et al., 2005). This test is believed to be under optimal conditions with short baselines between the airborne GPS antennas and the ground reference stations (GPS positioning errors are found to be the largest contributors to the overall error level by analysing different solutions).

For surveys in Arctic regions the error level is expected to be higher for most flight lines primarily because of poorer GPS conditions (less optimal satellite constellation) and longer baselines. In Hvidegaard and Forsberg (2002) a mean of 18 cm with a standard deviation of 12 cm is found when comparing the airborne (single beam laser) heights over a runway to a ground survey done by car. This indicates that the accuracy of the airborne laser height observations is in the order of one to two decimetres.

4 Studies of sea ice

When using altimetry over sea ice the reflecting surface will in general consist of a mixture of snow covered ice floes, ocean water between floes, and some surface freezing up creating new thin ice on the ocean. The ice floes are typically classified into two classes 1) first year ice, FY, which is ice formed during the recent winter and 2) multi year ice, MY, that has survived at least one summer's melt period. FY consists of very smooth floes with thickness less than 2 meters and MY ice is thickest (several meters) and has a more rough surface due to deformations of the ice field over several seasons. MY ice will consist of floes of different sizes with pressure ridges and open water (leads) between them. The deformations of the sea ice is dominantly controlled by wind-induced drift and bounded by the coastline. A comprehensive description of sea ice can be found e.g. in Wadhams (2000).



Figure 17. Photographs of typical sea ice conditions in Arctic Ocean

An altimeter measures the range between the instrument and the reflecting surface; the snow, ice or water surface. The reflected signal will come from a mixture of these reflectors for instruments with large footprints. Especially the space borne systems have large footprints, ICESat's are 60-70 m and CryoSat's footprints are 250 m along track and a few km wide.

A laser altimeter signal will be reflected off the top of the snow (if snow is present) or the water surface between floes. This is not entirely the case for radar altimetry. For Ku-band radars as SIRAL (and the D2P, ERS's RA, Envisat's RA-2, and JASON/Topex type radars) the reflecting surface will be the ocean surface and the top of the ice, but if snow is present the scattering surface is more uncertain. The dominant reflection is believed to come from the snow-ice interface but is depending on the dielectric properties of the snow above. Especially when the snow becomes wet when the temperature increases in spring/summer the snow will not be transparent to the radar signal. In this case the radar ranges to the snow surface or somewhere in the snow pack. Investigations are ongoing to resolve this uncertainty in radar altimetry over sea ice. Currently radar altimetry is not used for sea ice freeboard/thickness observations when melt occurs since no discrimination between ocean and ice reflections is possible (Peacock and Laxon, 2004).

4.1 Procedure for determining freeboard

The studies for this PhD started by analysing existing archived data from the 1998 survey north of Greenland. The single beam laser output was combined with INS and GPS information as outlined in chapter 2 to yield surface height measurements. From the analysis of these data it was obvious that further processing was needed. This led to the development of the lowest-level-filter technique. First results are presented in Hvidegaard and Forsberg (2002).

In short, the procedure can be described by the following observation equation for the sea ice freeboard, F , see also Figure 18:

$$F = h - r - N + e$$

Where h is the height of the airplane determined by GPS, r the laser range corrected for aircraft attitude from INS, and N the geoid height obtained from gravity measurements from other projects. Recently the Arctic Gravity Project (Forsberg and Kenyon, 2004) geoid model has been used. e consists of local deviations of the sea surface from the geoid and errors.

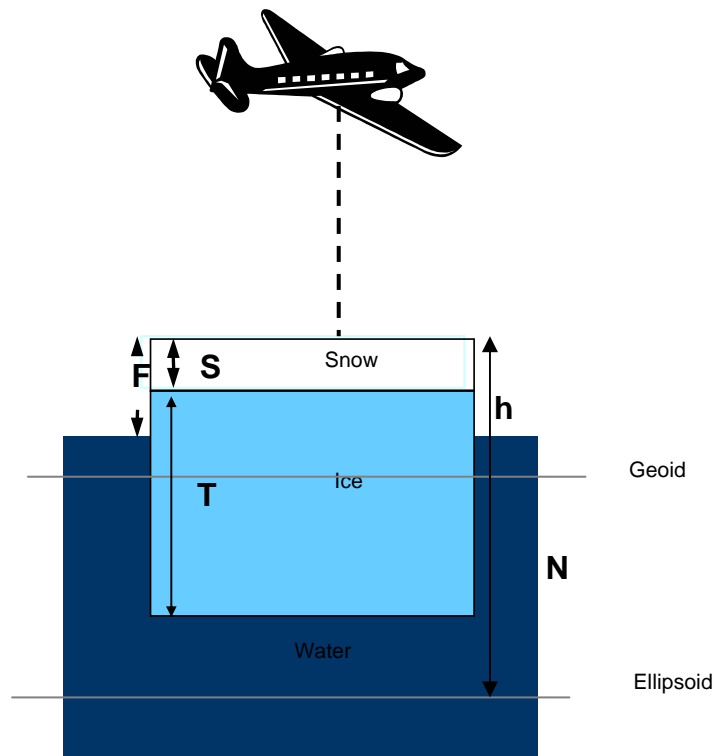


Figure 18. Principle of freeboard determination

e is removed/reduced by applying a “lowest level filter”. This technique determines e by a selection of the lowest values in the data assuming that these corresponds to the ocean surface or thin ice, followed by an interpolation between the selections to form the filter. This filter is then applied on the data to give the final freeboards. An example of raw data, filter, and freeboards can be seen in figure Figure 19 from Hvidegaard and Forsberg (2002). It is clearly seen that the filter corresponds to the lowest data values marked by I and II.

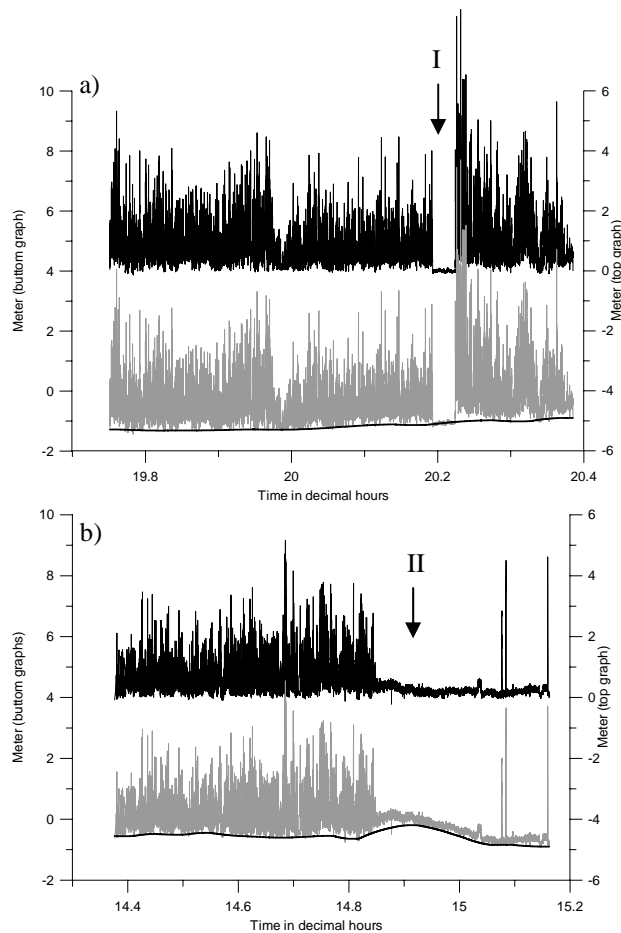


Figure 19. Example of height, freeboard and filter data. Grey curve: Freeboard heights from the equation above. Bottom black curve: Estimated sea surface used for filtering. Top black curve: Corrected freeboard heights after filtering (refers to right hand y-axis). Adapted from Hvidegaard and Forsberg (2002).

Figure 20 shows scanner swath data from the 2002 survey. Two different sea ice conditions are displayed. Left is seen a mixture of young smooth ice and old deformed ice. This can also be seen in the corresponding distribution of the data that is bimodal. The sample seen right is from almost entirely old sea ice; a small lead is seen to the south. The distribution of this section is much wider, reflecting the large range in ice thickness. The bottom plot displays the covariance for the two sections. The correlation length of the sections is found where the covariance is zero. The largest correlation length is for the old deformed ice (top right plot).

Besides the 1998 data set presented in the paper from 2002 this procedure has been used on the data from the more recent field campaigns.

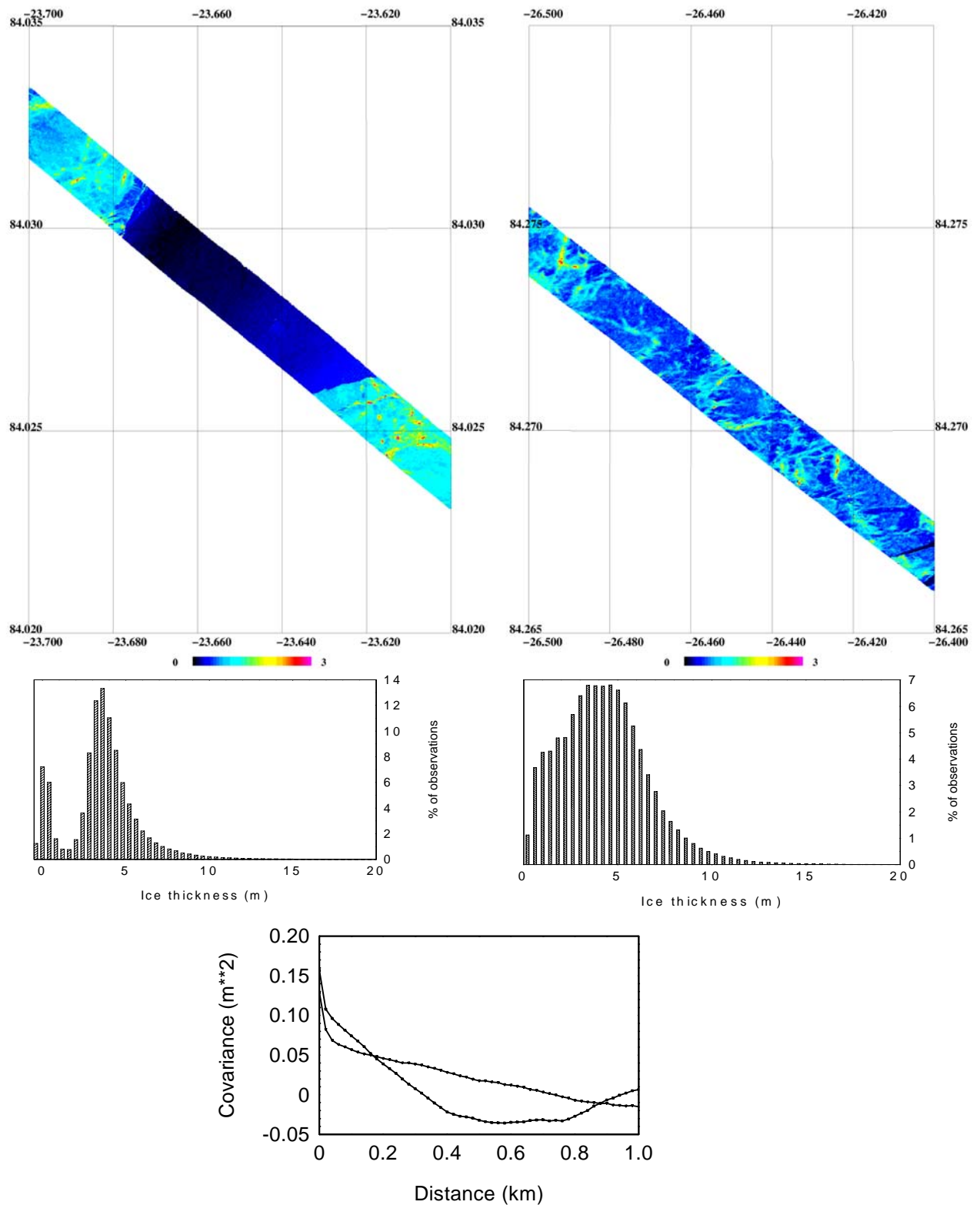


Figure 20. Example of data and statistics for scanner output. Top: Freeboard for approx. 1.5 km by 300 m swaths. Bottom: Statistics for 5 km sections including swaths from top figures. Conversion from freeboard to thickness is discussed next.

4.2 Estimation of sea ice thickness

From the freeboard data the total sea ice thickness (including snow cover depth) can be estimated using the assumption of an isostatic balance between ice including snow and the seawater. This is commonly described by a single factor, here denominated as the K-factor, given by the relation:

$$T = KF$$
$$K = 1 + \frac{\rho_i h_i + \rho_s h_s}{h_i(\rho_w - \rho_i) + h_s(\rho_w - \rho_s)}$$

where K is derived from the isostatic balance between the buoyancy of the ice plus snow from the sea water and the weight of the floe. See for instance Wadhams (1992) and Laxon (2003) for the use of this procedure. For the results presented here a seasonally dependent model for the Arctic Ocean, presented by Wadhams et al. (1992), is used (except for helicopter-borne electromagnetic system comparison near Polarstern see section 4.4.1). This model uses densities of ocean water of 1024 kg/m³, sea ice 915 kg/m³ and varying snow depth with season giving K ranging between 5.9 and 7.9 for the time of year of the obtained data sets. The accuracy of the method is expected to be around one meter (Hvidegaard and Forsberg, 2002) and most of the uncertainty comes from the K-factor. The snow depth and ice density is suggested to be the most uncertain parameters and especially snow depth, ice and snow densities are parameters that K is sensitive to.

Finding an appropriate K-factor is a research topic under development at the time of writing since it has profound influence not only on airborne observations as described here but is equally important for satellite measurements from ICESat and CryoSat (as well as other satellite altimetry missions).

During the different field campaigns samples of ice thickness, freeboard, snow depth and density have been taken to address this issue. Results are gathered in table 4.1.

Month/Year	Freeboard to Thickness Ratio	Min – Max Ratio	Model Ratio'
May/2002	5.6	5.3-6.6	5.9
May/2002	- *	3.0-3.5	5.9
April/2003	5.0**	-	6.0
May/2004	6.3	5.9-6.8	6.0

* Only two observations

** Based on observations of density of ice, 850 kg/m^3 and mean snow depth, 20 cm and assumed seawater and snow density, 1024 kg/m^3 , and 330 kg/m^3 .

'Model values for April/May: 915 kg/m^3 (ice), 1024 kg/m^3 (water), 330 kg/m^3 (snow), 35 cm (snow), and average thickness 3 metres.

Table 4.1. Observed freeboard to thickness ratio, K-factor, from drilling during 2002-2004 surveys.

These are very sparse data and are not representative for the Arctic Ocean in general but can serve as control for how good the method applies near the sampled sites. All these observations though show the same overall picture that the K factors from the in situ observations are lower than the model used. The reasons are not fully resolved and need more attention in the future. Observations from the Canadian SIMMS'92 experiment (Seasonal Ice Monitoring and Modelling Site) give values around 900 kg/m^3 for FY ice and $850\text{-}900 \text{ kg/m}^3$ for MY ice in Resolute Bay, Eastern Canadian Arctic. These numbers for the density of sea ice are lower than those used in the model and suggest that it is a parameter that needs to be examined further.

4.3 Ice thickness maps

Using the processing steps just presented above, on the different data sets, lead to snap shot representations of the observed sea ice fields for the particular time-of-year, see Figure 21. Bearing the seasonal change in-between observations in mind, comparing the different years will provide knowledge about the inter-annual variability of the observed regions.

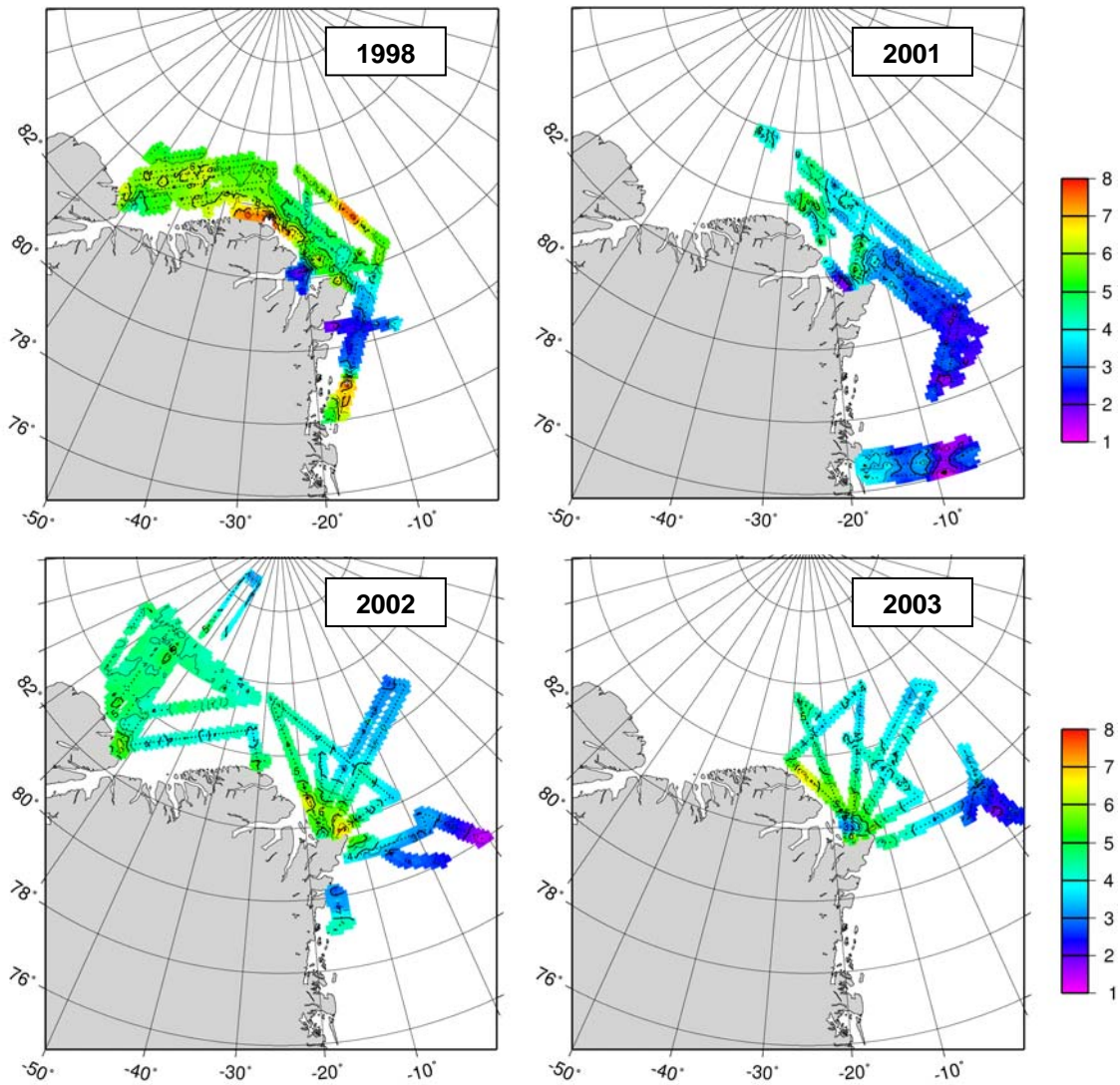


Figure 21. Sea ice thickness maps from the different surveys. The 1998 survey is from June, the 2001 from April/May, the 2002 from May, and the 2003 survey were done in April. (The freeboard to thickness ratios used is: 7.9, 5.9, 6.0 and 6.0 respectively).

For a first comparison of the four years of observations displays the average sea ice thickness for separate sectors. The sectors are 10 degrees in longitude by one degree in latitude. Red corresponds to 1998, black to 2001, blue to 2002, and green to 2003.

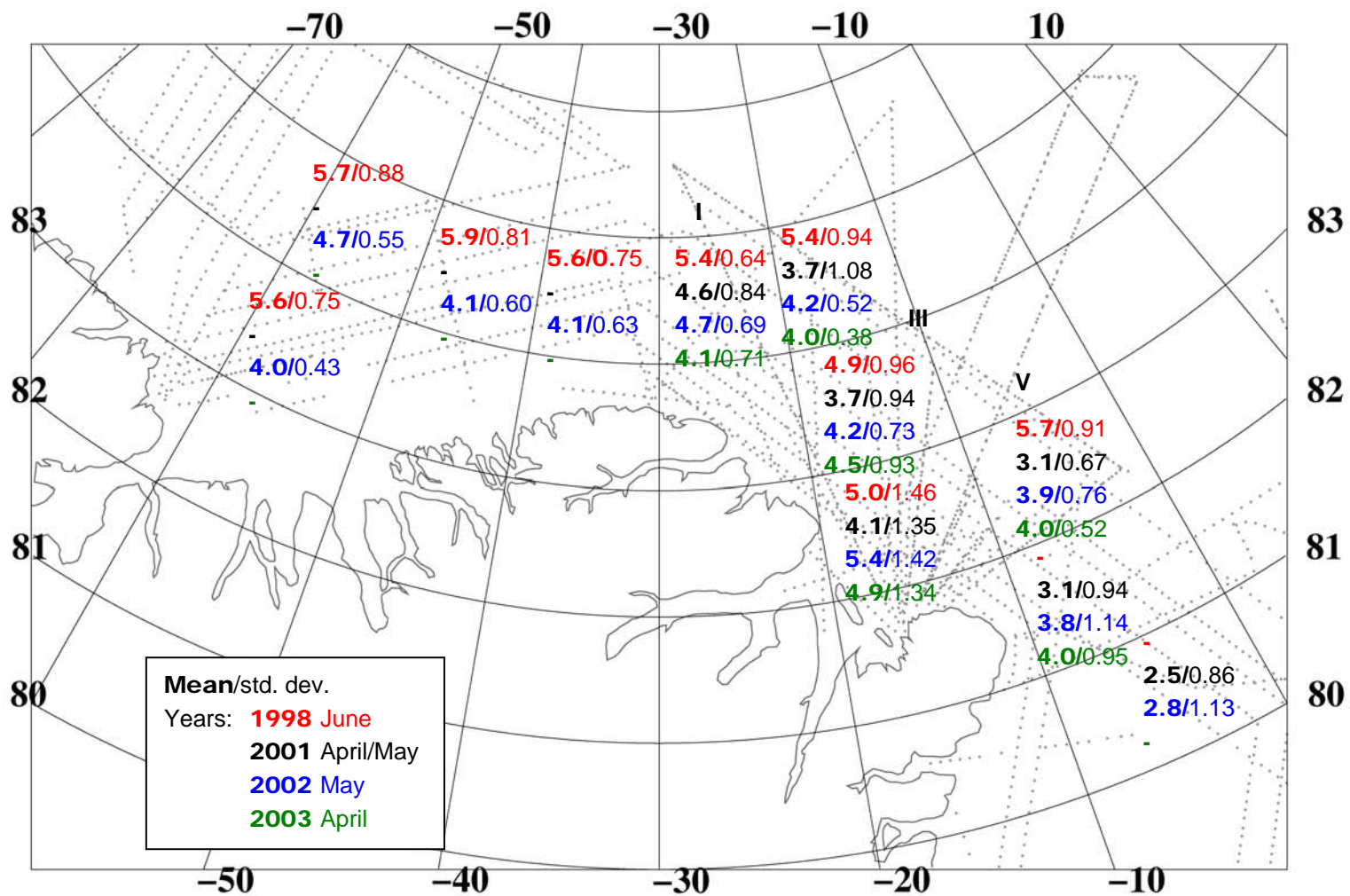


Figure 22. Average sea ice thickness and standard deviation of the averages for sectors bounded by latitude and longitude. The sectors are 10 degrees in longitude and 1 degree in latitude.

A large inter-annual variability is found with a change of the sector mean of more than one meter from year to year in several sectors. The overall picture seen is that the largest averages are found from the 1998 data and the 2001-2003 data have more comparable mean values. One reason for this may apparently be that the ice was thicker in 1998. Another could be that the model used for the freeboard to thickness ratio is less adequate during summer. The 1998 set is obtained in June whereas the 2001-2003 all have been measured during April and May before any melt sets in. No conclusions can be made as no independent sea ice thickness measurements have been found to validate the 1998 data.

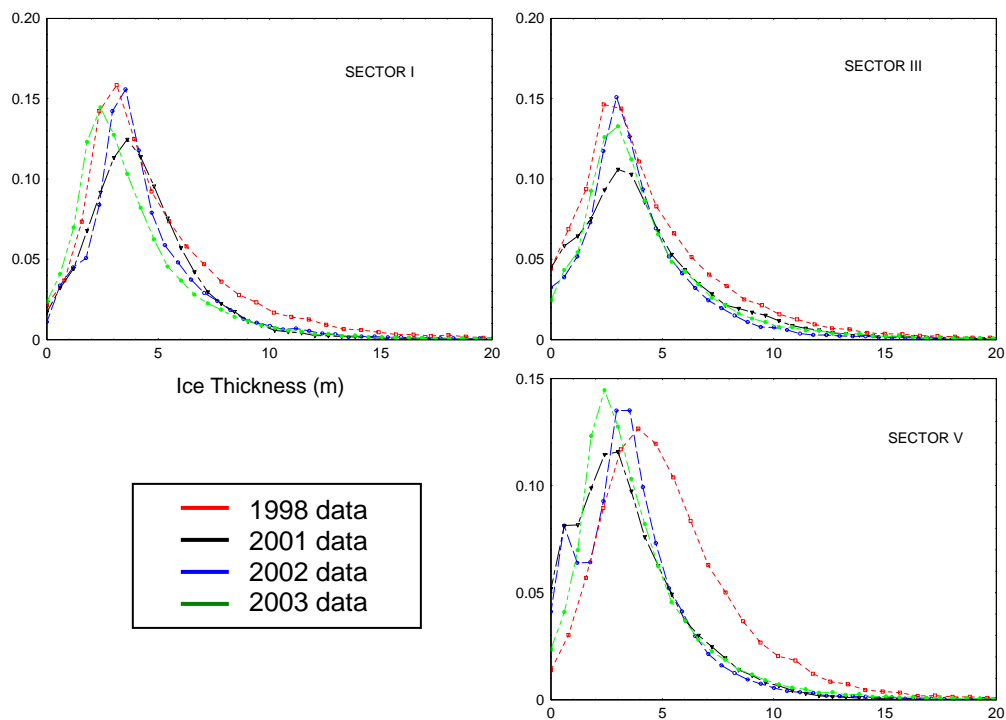


Figure 23. Examples of typical distributions.

Typical examples of distributions for the sectors are shown in Figure 23. A bimodal distribution exists for the southernmost sectors showing a mixture of thick multiyear ice (MY) and thin first year ice (FY) and open water near the ice margin. The northern sectors are all dominated by 3-4 meters thick MY ice.

Generally there is a narrower distribution in 2001-2003 than in 1998. This corresponds to a reduction in the amount of very thick ice. This corresponds to the overall picture of lower average values for the most recent years. The distributions remain peaked approximately at the same median value, which means that the most frequent values are almost unchanged. This is not the case for the southernmost sections showing much more variable conditions in the Fram Strait and East Greenland Current.

More inter-annual differences can be viewed when comparing yearly snapshots of sea ice thickness in Figure 21. In 1998 there was a large amount of thick ice along the North Greenland coast extending into parts of the Lincoln Sea towards the west. A typical polynia area is found just south of the northeast tip of Greenland (Nordøstrundingen) (See also Hvidegaard and Forsberg 2002).

The 2001 to 2003 data sets show generally thinner ice especially close to the coast. These data sets also extend the observed area towards the west and north in 2002 and east- and southwards in 2001.

One should bear in mind, when examining these plots, that the 1998 data set is from June, the 2001 from April/May, the 2002 set from May and the 2003 set is from April. Further more, the plots are based on observations from different days and adjacent tracks can be sampled with several days in-between where the ice field might have changed. The largest ice drifts are found in the Fram Strait.

The general ice conditions resembles the findings of others (e.g. Wadhams 2000) and show that the thickest ice is in the near-shore areas north of Greenland. From here there is a decrease towards the North Pole and also a decrease in mean thickness getting closer to the ice margin in the Fram Strait where more FY and open water is present.

4.4 Comparison to other types of data

In order to validate and further investigate the opportunities of the results from the DNSC laser altimeter system inter-comparisons have been done with other types of sea ice observations. The most valuable observations to compare with are independent measurements of both sea ice freeboard and thickness. One way to independently observe the sea ice thickness is by using an electromagnetic (EM) induction system.

4.4.1 HEM-system and related ground surveying

The 2003 field campaign was coordinated with the operations of the German research vessel Polarstern. Especially the drift phase where Polarstern was anchored to an ice floe for several days were useful for comparative studies between operations based on the ship and the airborne laser scanner surveys. From Polarstern both in situ work directly on the ice floe and helicopter borne measurements of the sea ice thickness was carried out. Comparison of data sets from the different platforms is used to validate the method of airborne laser scanning for sea ice thickness estimation and serve as a proof-of-concept for the method to be used for up-coming CryoSat validation.

The comparison of the DNSC system results and the data from fieldwork carried out from Polarstern, especially the helicopter borne electromagnetic induction system, the HEM, is presented in Hvidegaard et al. (2005). The main results are summarized below. Flight tracks and the position of Polarstern during the drift phase is shown in Figure 24.

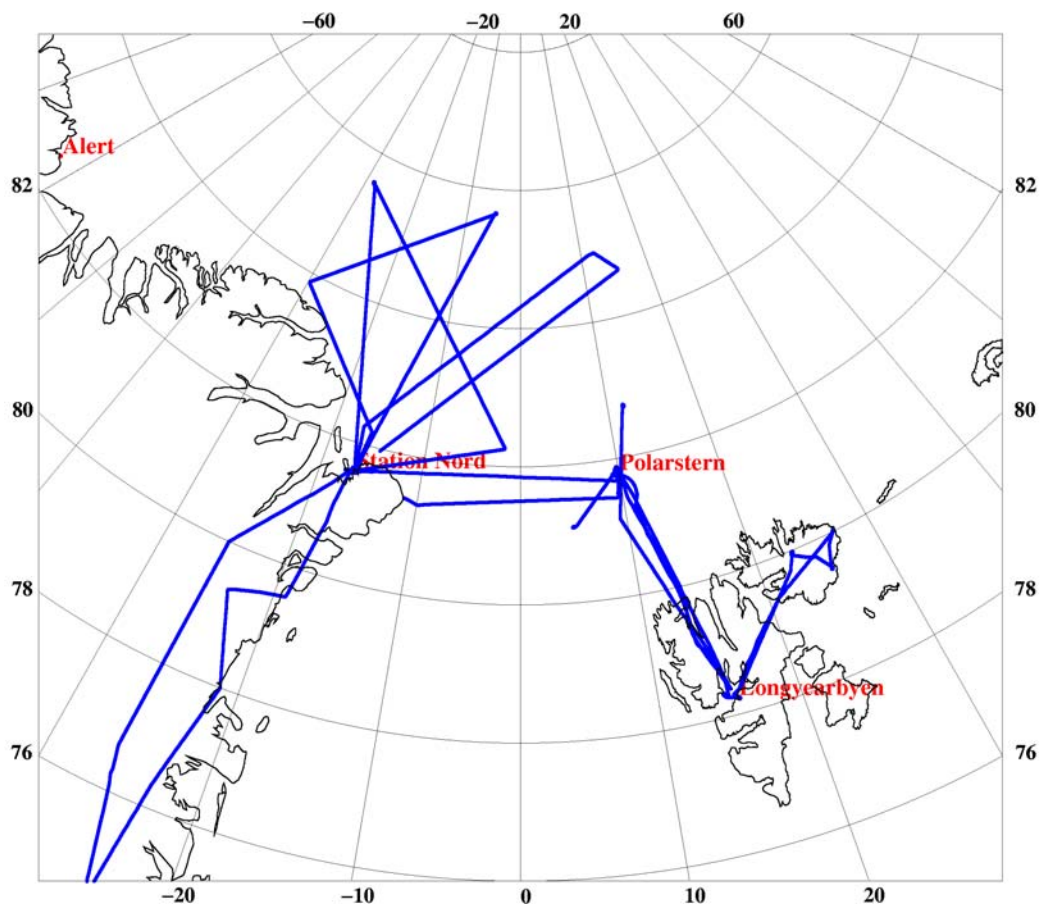


Figure 24. Flight tracks for CRYOVEX-2003.

During the Polarstern drift phase two coincident helicopter and Twin-Otter flights were performed. The two aircraft systems were flown on almost the same tracks in order to sample the same ice at the same time. Since the aircrafts fly with different ground speeds and the sea ice drifts in time, it was necessary to account for this in the flight planning. Photographs of the two aircrafts are shown in Figure 25.



Figure 25. Photographs of the two aircrafts, the Air Greenland Twin-Otter and a helicopter carrying the HEM-bird as a sling load.

The laser scanner data was analysed as described above except that the K-factor was derived from observations near Polarstern. The HEM system measures the sea ice thickness by inducing an electromagnetic field in the water below and around the ice and then observing the strength of the induced field. The field strength depends on the ice thickness and the total ice plus snow thickness is determined by profiling the top of the ice with laser altimetry.

The comparison of the two data sets shows very similar results. Figure 26 shows a small section from one of the flights. The two methods clearly measure the same ice and give comparable results. The differences between the average thickness from the two systems are within the expected accuracies for both coincident flights.

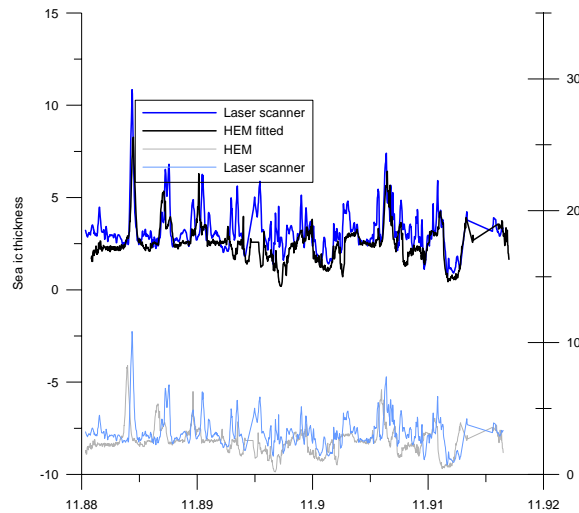


Figure 26. Small section of coincident HEM and scanner data: Example of data comparison showing high match of the features between the laser scanner derived sea ice thickness (blue) and the HEM determined thickness (black) after a small adjustment (top graphs) in addition to the drift corrected data (bottom graphs) (From Hvidegaard et al. 2005).

Data Type	Mean Thickness	Std. Dev.
Laser scanner April 11	2.12	1.56
HEM April 11	2.12	1.24
Laser scanner April 15	3.83/3.67*	1.77/1.66
HEM April 15	3.40	1.44
Laser scanner Circle: 50 m Drillings	3.14	0.59
Laser scanner pred. to EM31	2.62	0.29
EM31	3.15	0.99
	3.56	1.01

*The two means represent the two legs of the flight, forth and back to Polarstern respectively.

Properties are tabled for the selected coincident points of the data sets.

Table 4.2. Average sea ice thickness for different parts of the CRYOVEX-2003 coincident laser scanner, helicopter EM and ground surveys. Adapted from Hvidegaard et al. (2005).

During the campaign the floe that Polarstern was anchored to was surveyed with the laser scanner system, see Figure 27. This offered the opportunity to compare the dense laser scanner data to in situ ground observations done directly on the floe. The details of how the data sets have been compared are described in Hvidegaard et al. (2005). Comparing thickness from laser scanning to a grid of drillings shown by black dots on Figure 27 give a difference of 0.5 m. Comparison of laser scanning and ground based EM data (pulled over the ice in a kayak) results in a similar difference of 0.4 m. Both differences are well within the accuracy of the method estimated in Hvidegaard and Forsberg (2002) and suggest that the accuracy of the laser scanning derived sea ice thickness method is accurate on the ½ m level.

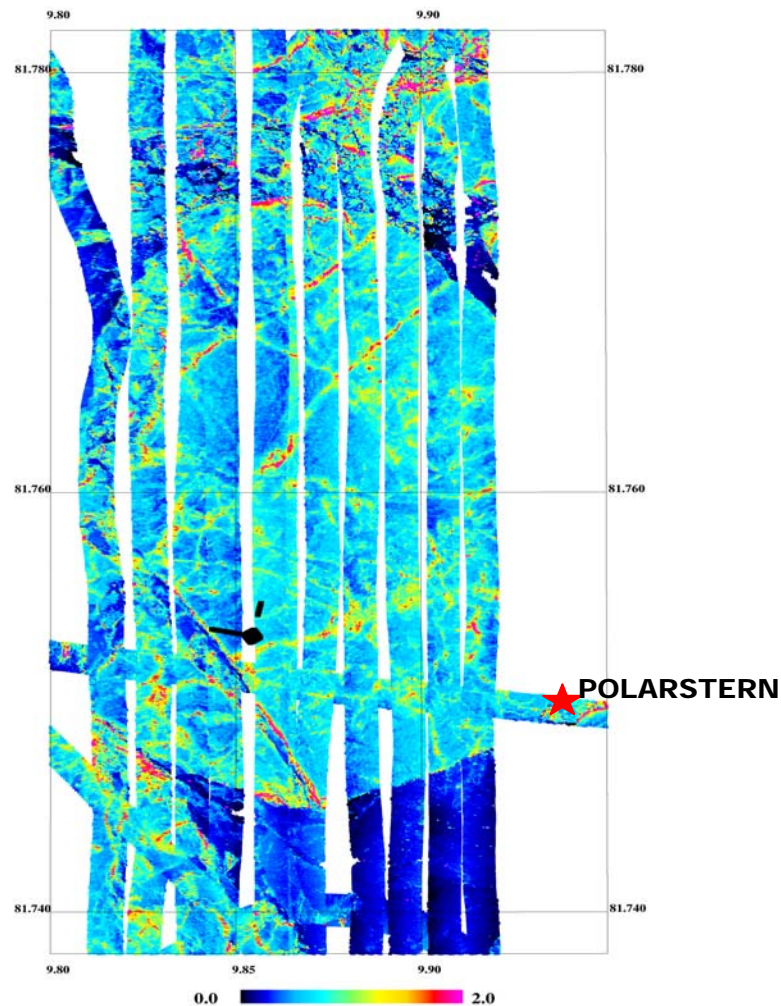


Figure 27. Dense laser scanner survey of the freeboard of the ice floe next to Polarstern. The survey was performed on April 17th 2003.

4.4.2 Oden webcam

Another way to validate the airborne laser system is by comparing it to thickness obtained from ice around an icebreaker. This was explored in 2002. The Swedish icebreaker Oden performed an oceanographic cruise in the Fram Strait and Greenland Sea in the period May 1st to June 8th, see Figure 28 for cruise track and photograph. DNSC (then KMS) had an automated web camera system mounted on the bridge of the ship taking pictures of the breaking sea ice at 20 seconds interval, 24 hours a day during the cruise. The images allow occasional measurements of ice floe thickness and snow cover depth when ice floe fragments accidentally turned vertical during ice breaking. Navigation data was provided by the navigation system onboard Oden. The Twin-Otter with the laser altimeter system over-flew Oden on two occasions during the 2002 survey, on May 6th and 9th, making a comparison of the two systems possible.

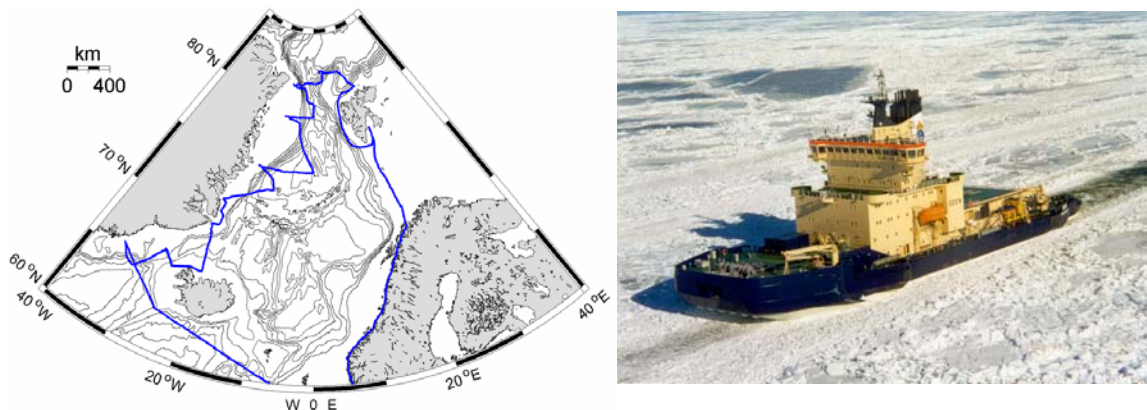


Figure 28. Oden cruise track, left, and photograph of the Oden icebreaker.

Occasionally the ice floes will be turned vertical when the ship breaks through the ice. The ice thickness can then be estimated by comparing to a “scale stick” mounted on the side of the ship, see Figure 29. Each mark on the stick corresponds to 50 cm, and 10% are added to the total thickness estimate in order to account for the distance from the stick to the ice surface. We estimate that the accuracy of this method is in the order of one or two decimetres.



Figure 29. Oden web camera examples. Scale stick is 2 m. Left: May 6th 08:46:22 Snow+ice=132 cm. Right: May 6th 10:29:22 Snow+ice=110 cm

Figure 30 shows the comparison of the laser derived 4 km along track ice thickness data (bullets) and the available ice plus snow thickness estimates from the Oden web camera images marked with crosses. A large difference is seen caused by the fact that the icebreaker only sails through the absolute thinnest parts of the ice cover, open or newly refrozen leads and thin ice avoiding old MY ice floes.

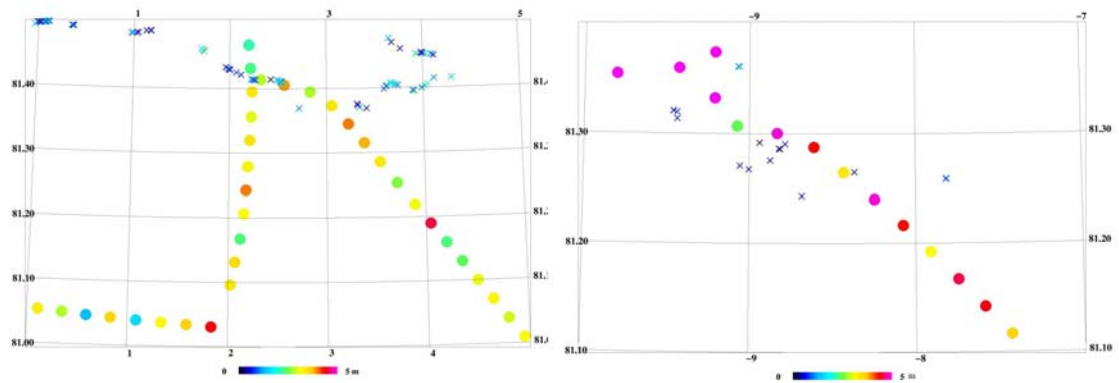


Figure 30. Comparison for May 6th, left, and May 9th, right. Bullets are 4 km average thickness estimates from laser and crosses are ice plus snow thickness from Oden web camera images.

Comparing the average thickness derived from the Oden images of 1.2 m for May 6th and 0.5 m for May 9th, to the distributions of the laser altimeter derived thickness is seen in Figure 31. The averages from Oden are marked by the dotted lines. For May 9th data from Oden corresponds to the thin-ice part of the distribution separated from the thicker ice. This is not seen in the May 6th data and no conclusions can be drawn from these analysis.

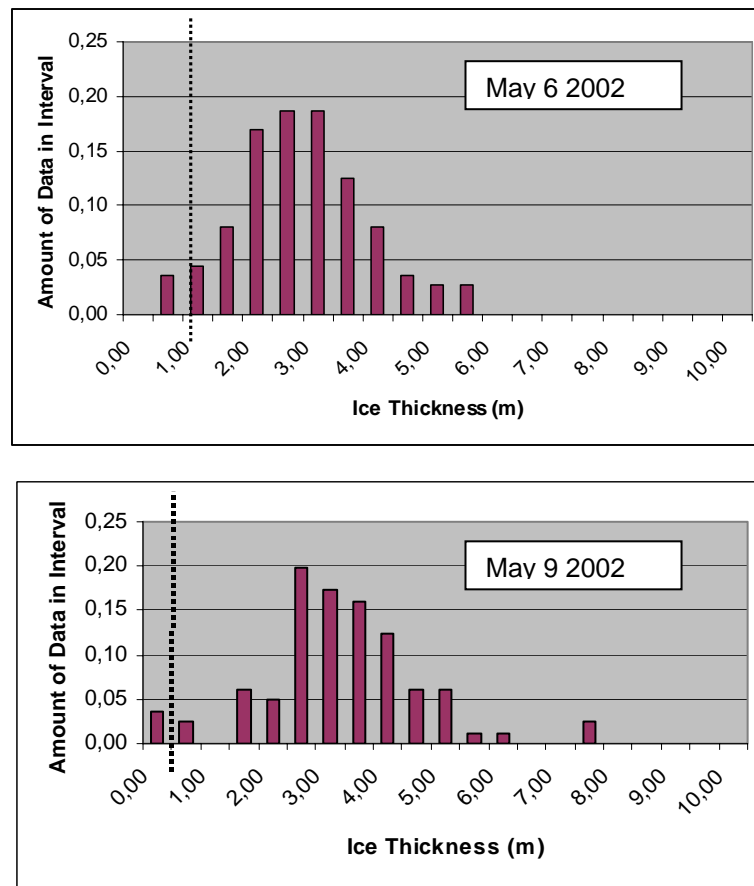


Figure 31. Comparison of mean sea ice thickness from Oden images to distribution of laser derived thickness.

Some estimates of snow depth from the Oden images have been obtained near the May 6th coincident tracks giving a mean snow depth of 32 cm. This corresponds very well to the 35 cm used in the model behind the K-factor used in the freeboard to thickness conversion of the laser data.

4.4.3 Radar versus laser incl. D2P

In order to study differences/similarities between the laser and radar systems different comparisons of the DNSC laser data to radar instruments have been investigated. First of all the 2003 campaign was in part dedicated to sample coincident laser and radar altimetry exploiting the co-mounted laser scanner and D2P radar systems on the Twin-Otter mentioned in section 2.2 and 2.3. Besides this, analyses have been done on laser data versus ERS-2 satellite radar altimetry (Giles and Hvidegaard, 2005) and laser data versus ENVISAT ASAR dual polarized imaging radar scenes (Toudal et al., 2005).

Laser scanning versus D2P radar altimetry

The coincident use of both the laser and the D2P systems from the Twin-Otter in the 2003 campaign provided many hours of co-sampled tracks. Areas with collocated radar and laser can be seen in Figure 32. Processing of the D2P data is very comprehensive and studies are still ongoing to utilize the D2P data. Only test sites have been fully analysed to give re-tracked height data. C. Leuschen (APL/JHU, USA) and L. Stenseng (DNSC) have carried out the data processing and the presented studies are a preliminary analysis done in cooperation with L. Stenseng.

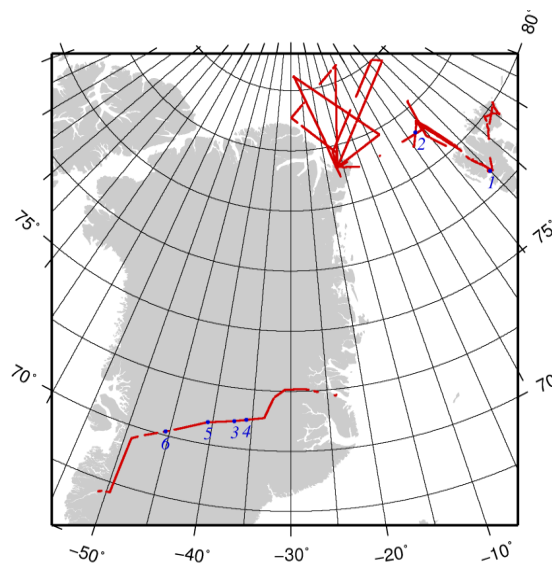


Figure 32. Map of collocated radar and laser altimetry for the 2003 CRYOVEX campaign.

The radar data processing by DNSC consist of the following steps (level 1b data is used, this is raw waveform data already coherently re-sampled exploiting the Doppler delay, (ref to APL report)),

- 1) Extract complex waveform data and construct amplitude and angle waveforms
- 2) Re-track amplitude waveforms to get height estimates
- 3) Determine offset between radar and laser
- 4) Ground reference re-tracked points using three-dimensional geometry

The D2P data has been re-tracked using a “half power of leading edge” algorithm. A “first peak maximum” algorithm was also found to be useful. Work still has to be done to find the optimal re-tracking method.

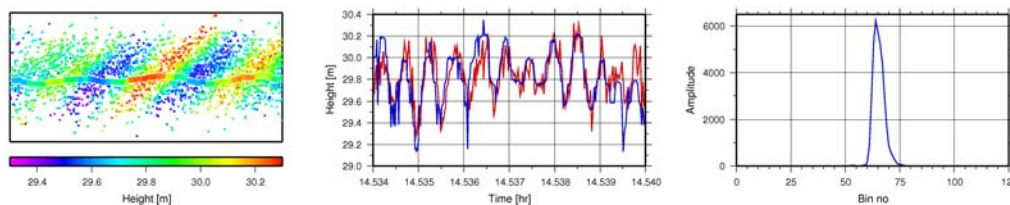


Figure 33. Offset test data. Left, elevation in colours: Laser swath, dots, and radar, squares. Centre: Elevation curves, laser in red and radar in blue. Right: Typical open water waveform.

Regarding point three, the off set determination was done over open water since both the laser and the radar signals are reflected off the water surface. A plot of the data is shown in Figure 33 from an open water area near Svalbard, marked by 1 on Figure 32. Some wave activity is clearly mapped.

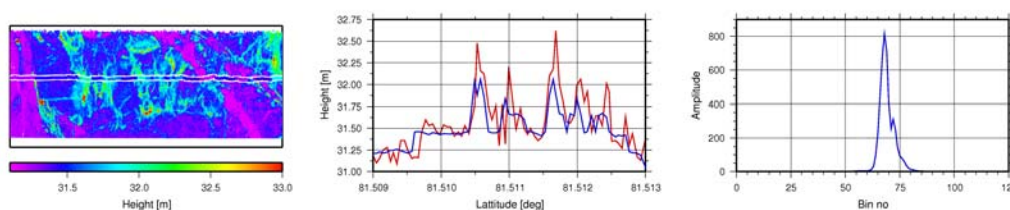


Figure 34. Sea ice comparison. Left, elevation in colours: Laser swath, dots, and radar, squares. Centre: Elevation curves, laser in red and radar in blue. Right: Typical sea ice waveform.

Figure 34 displays a comparison of radar and laser altimetry over sea ice, marked with 2 on Figure 32 (from the Fram Strait coincident laser and HEM flight described in section 3.4.1). Generally good correlation is seen, the laser though resolves the pressure ridges better because of the narrower footprint (laser footprint: 1 m and D2P footprint along track: 2-4 m).

The difference between the two height estimates has a standard deviation of 20 cm that is a measure of the error level and this is comparable to the vertical resolution of the D2P data (Raney and Leuschen, 2003). Over flat snow covered areas a slight difference between the radar and the laser derived heights is found (laser>radar) indicating penetration of the radar signal into the snow. This clearly needs more thorough investigation but might be exploited to estimate the snow cover depth. All comparisons of laser scanner and D2P derived heights have been done in a common reference frame referred to the ellipsoid i.e. prior to filtering of the laser data to avoid inducing additional error sources. The two data sets have large potential to provide more information about how a 13.9 GHz CryoSat type radar performs over ice and snow, and further analyses are proceeding.

Laser versus ERS-2 radar altimetry

This investigation addresses the issue of comparing the airborne laser and space borne radar altimetry measurements of sea ice freeboard. The full details are reported in Giles and Hvidegaard (2005). ERS-2 radar altimetry is compared to laser altimetry from the 2001 April/May campaign and the 2002 May campaign. The measurements used are the freeboard data i.e. heights of the ice or ice and snow above the sea surface.

The spatial scales for the comparison are derived from the laser data set and show correlation lengths in the order of 100 km. For the temporal scales, sea ice drift information from the International Arctic Buoy Program (<http://iabp.apl.washington.edu>) suggests that the data will be correlated within 4 days.

The data is compared by averaging the laser freeboards (higher than 5 cm to avoid sampling of open water) with a 100 km running mean and comparing to a mean of all radar points within 100 km and 4 days time separation. The resulting differences of the freeboards are shown in Figure 35 a and b. The figures also display average daily maximum 2 m temperature for the time period found from ECMWF operational data (<http://badc.nerc.ac.uk/data/ecmwf-op/>).

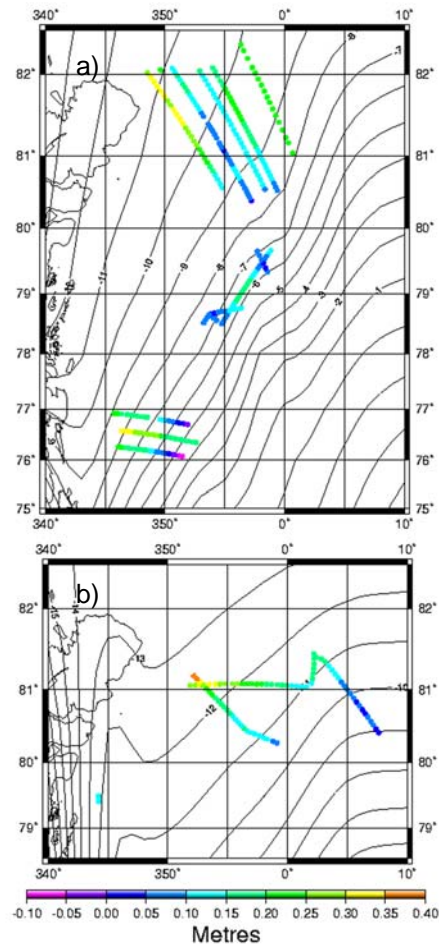


Figure 35. Laser freeboards minus radar freeboards in colours and mean maximum 2 m temperature contours.

As the snow depths are unlikely to be zero for the 100 km averages at this time of year in the study area, it can be assumed that snow is present on top of the sampled ice. In this case the radar signal will penetrate the snow and be reflected by the ice beneath if no melt occurs. If melt has begun the reflection is expected to come from somewhere between the snow surface and the ice surface. In both cases the laser will be reflected by the interface between air and snow. Therefore the differences in the figures can be a mixture of different average snow depth and varying penetration into the snow layer due to changing surface temperatures.

The general feature to notice, is that there is a negative correlation between gradients in the differences and the temperature gradients. The largest differences are found close to the east coast of Greenland with values in good correspondence with snow depths suggested by the climatology of Warren et al. (1999). For the 2002 data a good agreement is also found comparing to the mean snow depth of 32 cm from the Oden web camera images near 81.5N and 2-3E where the difference between laser and radar is approximately 25 cm.

Laser scanner swath data versus ENVISAT ASAR

In connection with the 2003 campaign Wide Swath (WS) ENVISAT, Advanced Synthetic Aperture Radar (ASAR) scenes were acquired. These were ordered to exploit the ability of the SAR data to monitor the sea ice drift in the experiment region in near real time. In addition a set of high resolution Alternate Polarization (AP) scenes were ordered. Some of the acquired ASAR AP scenes have been compared with freeboard height data derived from the DNSC laser scanner system and presented in Toudal et al. (2005). The main results are outlined next.

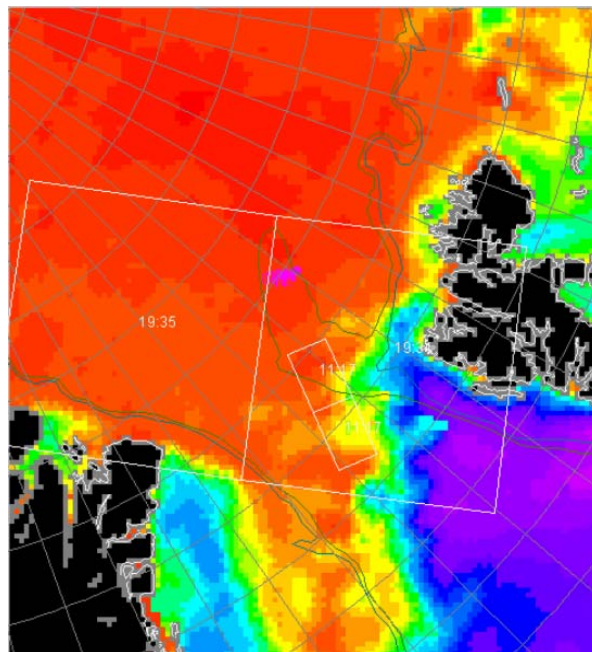


Figure 36. QuickSCAT scatterometer image of the Fram Strait on April 11, 2003, showing in white the approximate location and coverage of the ENVISAT ASAR WS and AP images on that day from Toudal et al.(2005).

A good overlap between ASAR data and laser altimetry was collected on April 11th 2003 and the coverage of the ENVISAT ASAR WS and AP images is displayed in Figure 36 as white boxes on top of a QuickSCAT scatterometer image from the same day. The dual polarization of the ASAR high resolution data provides the opportunity to plot the data as a false colour composite (of intensity, hue and saturation, see Toudal et al., 2005, section 3). Comparing this to laser scanner freeboard swath data shows a very good match of features, see Figure 37. The blue areas in the laser data correspond to thin ice and the green colours to thicker ice. The image floe boundaries are found from the ASAT and overlaid on the laser swath to emphasize the comparison.

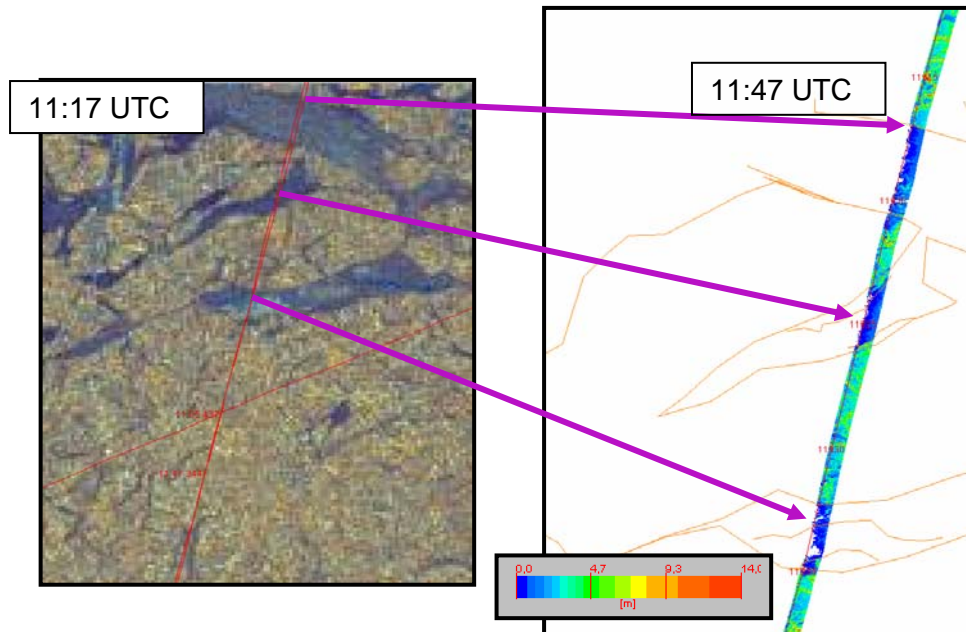


Figure 37. False colour composite of ASAR data and laser scanner freeboard swath (Adapted from Toudal et al., 2005)

Comparing the ASAR backscatter (both for parallel and cross polarization) to laser freeboards show that SAR can discriminate between two classes, thin lead ice and thicker MY ice in this area. No apparent relationship between backscatter and ice thickness is seen within each class. This is in good agreement with previous results from the airborne EMISAR polarimetric observations presented by Thomsen et al. (1998).

4.5 Summary of sea ice results

DNSSC laser system delivers high resolution sea ice freeboard data providing analysis opportunities on scales ranging from few metres to hundreds of kilometres.

Repeated observations can be used to monitor sea ice covered regions as have been done since 1998 in the area of the Arctic Ocean north of Greenland.

Despite the limitations in the used method to estimate sea ice thickness especially from uncertainties in the conversion from freeboard to thickness, we see a significant decrease in the ice thickness from 1998 to 2001-2003. Whether this is caused by a general thinning of the Arctic ice cover or a part of the natural variability in the area cannot be concluded from these observations. What can be stated is that the year-to-year difference is large - in the order of 1 meter in mean thickness in the study area.

The primary two effects that can cause the change in thickness we see from the observations are: Redistribution of ice in the Arctic Ocean and increased melting of the sea ice during the short arctic summer season (June-August).

The system is validated through comparisons to ground surveys and comparison to the helicopter borne EM system. The combination of in situ ground observation, HEM and laser scanner airborne observations will be able to bridge the local studies to the regional observations from satellites such as CryoSat. This combination is a promising method to be used for CryoSat validation, especially when the measurements are extended with the ASIRAS radar system (a SIRAL copy to be flown on small aircrafts).

To average the high resolution airborne data to scales of radar altimeter footprint, still more analyses need to be done on how. Tests with SIRAL data processing simulator with laser scanner heights as input are being done by D. Wallis (UCL, UK, personal comm.).

Comparisons of laser and radar show new opportunities to observe sea ice snow covered thickness and explore differences in scattering/reflecting surface.

5 Studies of land ice

Inland ice consists of the great ice sheets of Greenland and Antarctica and local ice caps and glaciers around the World. The investigations under this study have been focused on the Greenland Ice Sheet and marginal glaciers. On two occasions local ice caps have been surveyed, the Geikie ice cap, East Greenland, and the Austfonna ice cap in Svalbard.

A standard model of an ice cap divides it into different zones. Figure 38 sketches this with the common terms used. The description is based on the formulation by Patterson (1994). Starting from the top these are, the dry snow zone where no surface melt occurs. The dry snow zone can only be found in the interior of Greenland and Antarctica where the mean annual temperature is -25°C or below. Then the percolation zone, where the summers melt water percolates down in the ice and refreezes. The wet-snow zone is characterized by the fact that all the ice is at zero degrees at the end of the summer and last, the super imposed ice zone consists of old ice and refrozen melt water. The ice cap is divided by the equilibrium line into the accumulation area with net accumulation of snow and the ablation area where mass is lost by ablation of melted ice and snow.

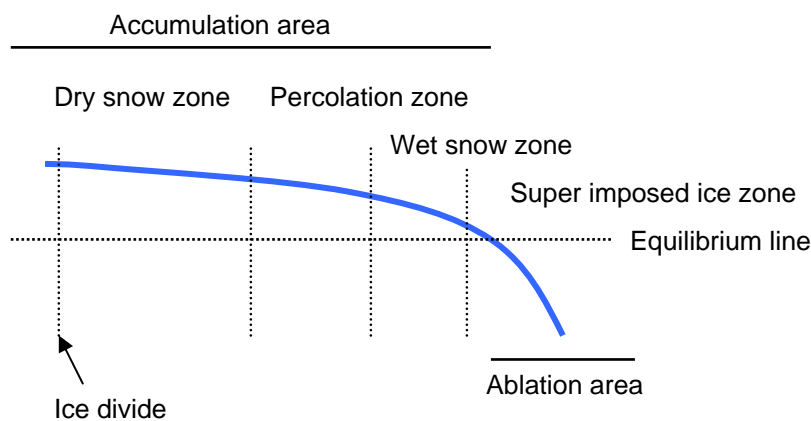


Figure 38. Ice cap zones.

For climate change studies it is important to monitor the “state of health” of the ice caps and glaciers. The advance or retreat of glacier terminus is not providing the whole picture and it is much better to measure the change in total mass if possible.

These studies are called mass balance studies. One way to do this is by mapping the elevation change and combining this with knowledge and assumptions about average densities and flow patterns. Mass balance studies by Krabill et al. (2004) using airborne laser altimetry and Forsberg (pers. comm.) using GRACE gravity change observations show a net average loss of 60 and 55 km³/yr respectively and the observations by CryoSat will be used to monitor changes in the future.

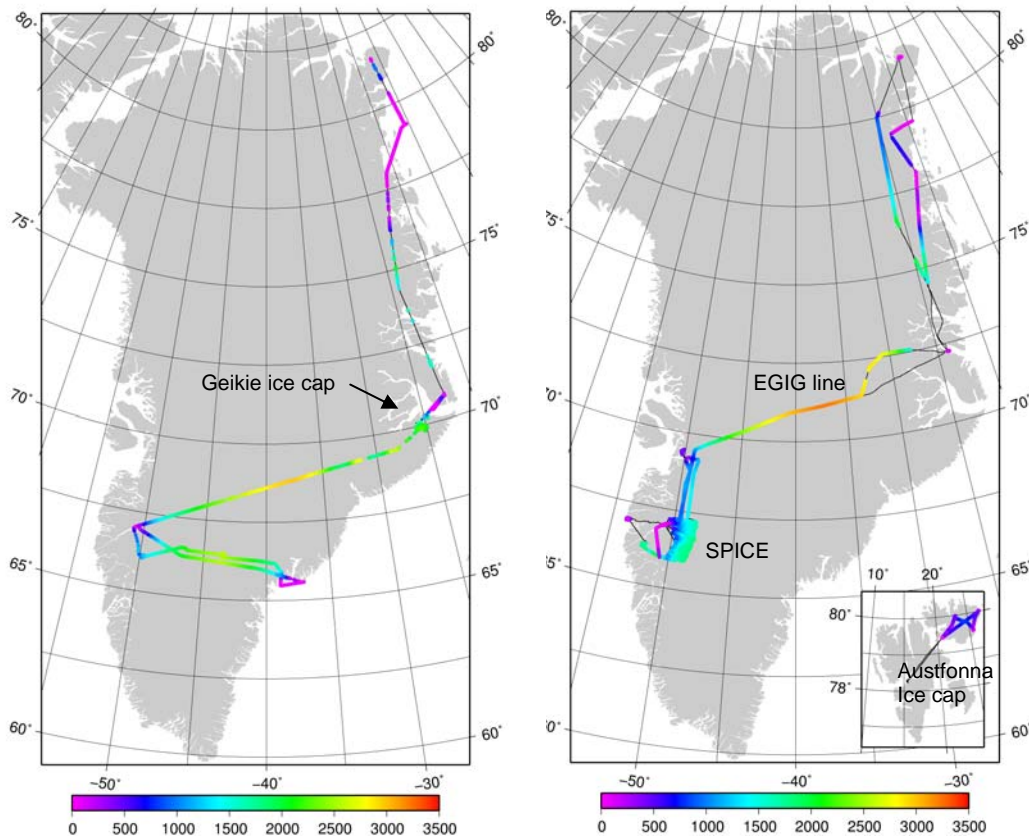


Figure 39. Inland ice laser data from 2002, left, and from 2003, right.

5.1 Repeated observations

During the surveys in 2002 and 2003 several hours of laser scanning were done over inland ice areas in Greenland and the Austfonna ice cap in Svalbard (inserted figure in Figure 39) was mapped in 2003. Some lines were repetitions of previously surveyed areas but most were aimed at being repeated in the future. Figure 39 gives an overview of the obtained elevation data.

The southernmost part in Figure 39, right, is from the EU fifth framework project SPICE. This area was surveyed with the DNSC laser scanner system and Danish Technical University's ice penetrating radar in August 2003. The same area was mapped with the single beam laser in 2000. Preliminary results from comparing the

two data sets are presented by Ahlstrøm et al. (2005) and show differences generally between 0 and 2 metres with the most significant change near the ice margin, 2003 elevations lower than 2000. The accuracy is still not finally resolved but is expected to be better than 0.75 metres. The intention is to use this data for local mass balance studies and the area will be re-surveyed in 2005. This type of study shows the opportunities available using the laser scanner system for detailed monitoring of an area.

The line crossing the Greenland Ice Sheet in 2003 is called the EGIG line. This is one of the focus areas for the CryoSat cal/val campaigns. The EGIG line is named by an expedition in the 1950th's (Meddelelser om Grønland, 1977), called Expédition Glaciologique au Groenland, and old elevation data exist from this, but these needs proper referencing before it is useful. The line was also mapped in 2004 and elevations from both years are shown in Figure 40. In 2004 different glaciological measurements were done on sites along the line and synthesis of the data is intended.

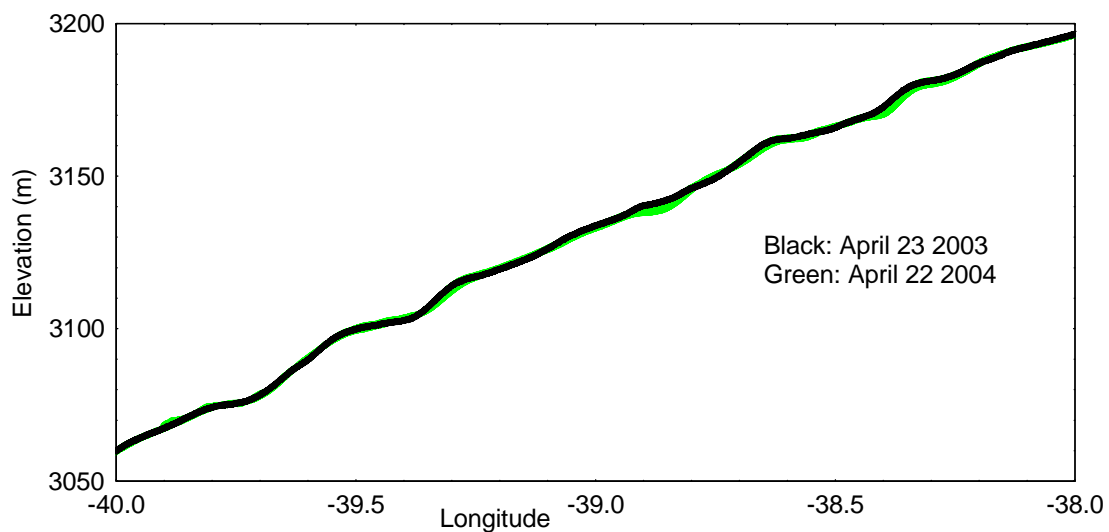


Figure 40. EGIG line 2003 and 2004

The 2002 survey of the Geikie ice cap, marked on Figure 39, was done in order to re-verify the lines from a survey in 1997 (Nielsen, 2001). There are still some unresolved problems with parts of the 2002 data set and therefore only a preliminary comparison can be presented. The difference between the elevations from the two data sets have been found by selecting the data points in the 2002 data around the 1997 data points (within 150 metres) and estimating a height value using weighted means interpolation.

The differences are shown in Figure 41, 1997 heights minus 2002. The accuracy of the two data sets are not fully analysed but errors are expected to be largest for the 1997 data because only an experimental INS system was used to determine the aircraft attitude angles. The accuracy of the differences is expected to be less than one meter. The comparison shows that there are no significant changes of the ice caps interior over the time period. The north-western margin may have changed but the larger difference there can also be an artefact of the differencing method (there can be up to 150 metres between observed elevations).

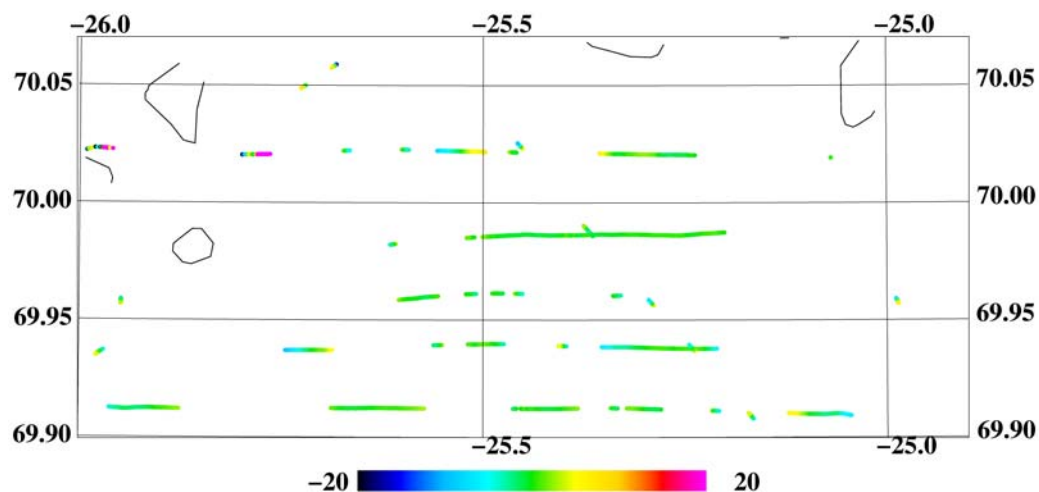


Figure 41. Geikie preliminary comparison. Elevation differences, 1997 minus 2002.

Much more change analysis can be done after repeating surveys as planned for CryoSat cal/val campaigns. Already with the 2004 and 2005 data sets some of the lines from previous surveys have been re-flown and comparisons are in progress.

5.2 Laser versus radar

The mapping with laser and radar altimeters during the 2003 campaign provided data both over sea ice and inland ice, see Figure 32 section 4.4.3. As for sea ice the radar scattering surface will depend on the snow/firn properties. Among these are liquid water content, grain size, density variations and ice layers and lenses expected to have significant impact.

Some examples of coincident laser scanner and D2P data have been compared. The processing and internal calibration have been done as outlined in section 4.4.3. In Figure 42 an example near Summit in the dry snow zone, marked by 3 in Figure 32, is seen. The laser heights are about one metre higher than the radar derived heights indicating the size of the radar penetration. The same size of difference between laser and radar results is found in other examples along the EGIG line, marked with 3-6 in Figure 32. This does not seem to correlate with the accumulation variations across the ice sheet found by Ohmura and Reeh (1991) and further investigations are needed before any conclusions can be made.

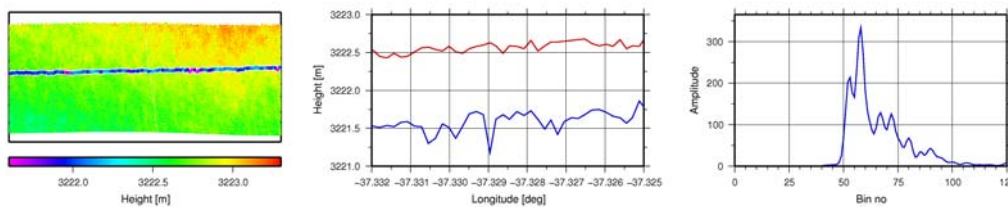


Figure 42. Comparison of laser (swath, background, in left plot, red line in centre plot) and radar elevations near Summit, Central Greenland. Radar elevations and a typical waveform are shown in blue in centre and right plots.

Figure 43 shows another example of D2P radar results also from the dry snow zone. The colours correspond to normalised return power. Different layers are clearly seen. This may be the yearly accumulation layers and might be used to study the layering of ice caps over larger scale than possible with ground based measurements.

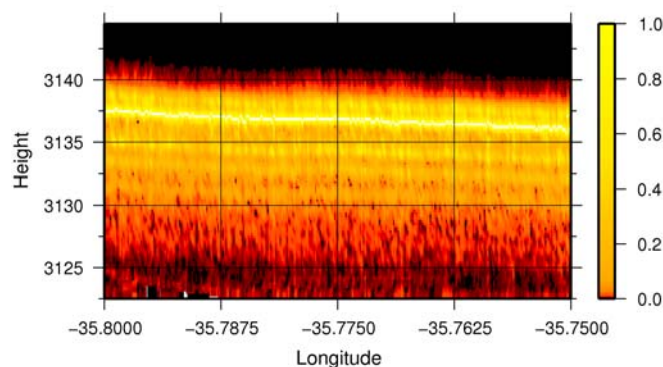


Figure 43 Radar return power and corresponding elevations (m) along EGIG line showing possible accumulation layers in the dry snow zone.

5.3 Summary of land ice results

Some examples of how the DNSC laser scanner system can be used to monitor changes of the ice have been presented. Many more investigations of this kind can be made in the future both with existing data and by repeating line already surveyed. The investigation for this PhD has been limited by time constrains. The CryoSat cal/val program will aim at re-flying some of the surveyed areas and the result can then be used to validate change result from the satellite.

Preliminary results have been shown from comparisons of laser scanner and D2P (CryoSat type) radar data. Over dry snow, penetration of the radar signal is found as expected. Much more data is gathered, also over different parts of the ice sheet, and further comparison may provide information about penetration in these areas.

Different layers are seen in the D2P data and similar results are found analysing ASIRAS data (R. Cullen, ESA-ESTEC, personal comm.). The origin of these reflections and whether similar results will be obtained by CryoSat will be very interesting to investigate.

6 Conclusions

Methods for CryoSat validation have been evaluated and the main results have been summarised in the end of chapter 4 and 5. The conclusions are:

- The DNSC system is very useful for mapping of inland ice heights and sea ice freeboards. By combining these measurements with radar altimetry and surface in situ observations, valuable validation experiments can be carried out in support of the CryoSat mission.
- For sea ice we have proved the concept of combined airborne laser and radar altimetry and helicopter-borne electromagnetic sea ice thickness observations. This validation concept was refined during the 2005 campaign and is planned for the actual validation campaign after CryoSat is launched.
- An extensive data set for several years and different ice covered ocean and land areas has been obtained. Parts of the laser scanner data have already been used to simulate the observations of CryoSat.
- The experiment results themselves are valuable data sets and provide many opportunities to study different characteristics of the Cryosphere.

Still many investigations are obvious for future research with the gathered data sets and newer and planned surveys. The most essential will be the fieldwork planned to take place when CryoSat is launched.

Answering some questions often reveals new ones and some ideas and needs for more investigations have been formed during the work presented here. The resulting recommendations for future research are listed below. More thorough investigation are needed of:

- The sea ice parameters used for the method of converting sea ice freeboard to thickness. Both a compilation of existing records of observations and new experiments will be useful.
- The absolute accuracies of the airborne altimetry system. It is especially important for inland ice studies.
- Accumulated snow depth mapping combining laser and radar. This will both be possible from airborne coincident operations and from space with the combination of CryoSat and ICESat.

- Statistics of sea ice ridges and leads and the effect on CryoSat sampling. One possibility is to use the detailed laser scanner swath data and from this quantify the metre-scale surface roughness.
- Sea ice thickness results from the laser scanner system in comparison to climate models.
- Possible observations of accumulation layers with Ku-band radars seen over dry-snow-zone samples. This will only be recognizable in the raw data, for instance level 1b from CryoSat.
- Inland ice height changes. This has only been limitedly explored under this PhD studies because of time constraints. Many flight hours of data need to be examined.

Finally, one should not forget to mention the future investigations of the result from the CryoSat Mission itself.

BIBLIOGRAPHY

Ahlstrøm, A. P., N. Reeh, L. Stenseng, R. Forsberg: Elevation change of the West Greenland ice-sheet margin near Kangerlussuaq 2000-2003, *Proceedings IASC-WAG Meeting*, Switzerland, 2005.

Andersen, C. J., N. S. Dalå, R. Forsberg, S. M. Hvidegaard, K. Keller and L. Stenseng: Airborne laser-scanning survey from the Wadden Sea, Denmark, *DNSSC Technical Report*, 2005.

Drinkwater, M. R., R. Francis, G. Ratier, and D. J. Wingham: The European Space Agency's Earth Explorer Mission CryoSat: Measuring Variability in the Cryosphere, *Annals of Glaciology*, vol. 39, 2004.

European Space Agency (ESA) and University College London (UCL): CryoSat Calibration and Validation Concept, *European Space Agency (CS-PL-UCL-SY-0004)*, 2001.

European Space Agency (ESA): CryoSat Mission and Data Description, European Space Agency, 2001.

European Space Agency (ESA): CryoSat Calibration and Validation Plan, *European Space Agency*, 2003.

Dalå, N. S., R. Forsberg, K. Keller, H. Skourup, L. Stenseng, and S. M. Hvidegaard: Airborne lidar measurements of sea ice north of Greenland and Ellesmere Island 2004 - GreenICE/SITHOS/CryoGreen/§76 projects Final Report, *DNSSC Technical Report*, 2005.

Forsberg, R., A. Olesen, and K. Keller: Airborne Gravity Survey of the North Greenland Shelf 1998, *KMS Technical Report*, NO. 10, 1999.

Forsberg, R., A. V. Olesen, K. Keller, and M. Møller: Airborne Gravity Survey of Sea Areas Around Greenland and Svalbard 1999-2001, *KMS Technical Report*, NO. 18, 2002.

Forsberg, R., K. Keller, S. M. Hvidegaard and A. V. Olesen: ESAG-2002, European gravity and lidar survey in the Arctic Ocean, *KMS Technical Report*, NO. 21, 2003.

Forsberg, R. and S. Kenyon: Gravity And Geoid in The Arctic Region – The Northern Polar Gap Now Filled. 6 pp., *Proceedings International GOCE Workshop*, ESA-ESRIN, March 2004.

Fu, L. L. and A. Cazenave: Satellite Altimetry and Earth Science: A Handbook of Techniques and Applications, *Academic Press*, 2001.

Giles, K. A. and S. M. Hvidegaard: Comparison of space borne radar altimetry and airborne laser altimetry over sea ice in the Fram Strait, *Int. J. of Remote Sensing*, in press, 2005.

- Hvidegaard, S. M. and A. V. Olesen: GreenICE 2005. Airborne laser scanning of sea ice north of Greenland, *DNSSC Field Report*, 2005.
- Hvidegaard, S. M. and R. Forsberg: Sea-Ice Thickness from Airborne Laser Altimetry over the Arctic Ocean North of Greenland, *Geophys. Res. Lett.*, 29(20), 1952, 2002.
- Hvidegaard, S. M., R. Forsberg, C. Haas, and A. Pfaffling: Comparison of sea-ice thickness measured by laser scanning and electromagnetic methods in preparation for ESA's CryoSat mission, submitted to *Int. J. of Remote Sensing*, 2005.
- Keller, K., S. M. Hvidegaard, R. Forsberg, N. S. Dalå, H. Skourup and L. Stenseng: Airborne lidar and radar measurements over sea-ice and inland ice for CryoSat validation: CRYOVEX-2003 final report. *KMS Technical Report*, NO. 25, 58p, 2004.
- Krabill, W., et al.: Greenland Ice Sheet: Increased coastal thinning, *Geophys. Res. Lett.*, 31, L24402, 2004.
- Laxon, S. W., N. Peacock and D. Smith: High Inter-Annual Variability of Sea Ice Thickness in the Arctic Region, *Nature*, 425, 947-950, 2003.
- Meddelelser om Grønland, Bind 173, *Arnold Busck*, 1977.
- Nielsen, C. S.: Topography and Surface Velocities of an Irregular Ice Cap in Greenland Assessed by means of GPS, Laser Altimetry and SAR Interferometry, *KMS Technical Report*, NO. 11, 81p, 2001.
- Ohmura, A. and N. Reeh: New precipitation and accumulation maps for Greenland, *Journal of Glaciology*, Vol. 37, NO. 125, 1991.
- Olesen, A. V.: Improved airborne scalar gravimetry for regional gravity field mapping and geoid determination, *KMS Technical Report*, NO. 24, 2003.
- Patterson, W. S. B.: The Physics of Glaciers, Third Ed., *Butterworth-Heinemann*, 1994.
- Peacock, N. R. and S. W. Laxon: Sea surface height determination in the Arctic Ocean from ERS altimetry, *J. Geophys. Res.*, 109, C07001, 2004.
- Raney, R. K.: The delay/Doppler radar altimeter. *IEEE Trans. Geosci. Remote Sensing*, 36 (5), 1578-1588, 1998.
- Raney, R. K. and C. Leuschen: Technical support for the deployment of radar and laser altimeters during LaRA 2002. Final report. *European Space Agency (ESA Study Contract ESATEC 16306/02/NL/SF)*, 2003.
- Rothrock, D. A., Y. Yu, and G. A. Maykut: Thinning of the Arctic sea-ice cover, *Geophys. Res. Lett.*, 26, 3469-3472, 1999

Shokr, M. E. and N. K. Sinha: Physical, Electrical and Structural Properties of Arctic Sea Ice Observed During SIMMS'92 Experiment, *Research Report* NO. CARD 95-005, Environment Canada, 1995.

Thomsen, B.B., S. Nghiem, R. Kwok: Polarimetric C-band SAR observations of sea ice in the Greenland Sea, *IEEE International Geoscience and Remote Sensing Symposium Proceedings*, Vol 5, p 2502-2504, 1998.

Toudal, L., K. Kloster, S. M. Hvidegaard, K. Keller, and R. Forsberg: Comparison of Single and Dual Polarized ENVISAT ASAR Data with Laser Scanner Data of Sea Ice Freeboard in Fram Strait, *Proceedings of the 2004 Envisat & ERS Symposium, Salzburg, Austria September 2004, ESA SP-572*, 2005.

University College London (UCL): CryoSat Science and Mission Requirements, *European Space Agency (CS-RS-UCL-SY-0001)*, 1999.

Wadhams, P., W. B. Tucker, W. B. Krabill, R. N. Swift, J. C. Comiso, and N. R. Davis: Relationship between sea ice freeboard and draft in the Arctic Basin, and implications for ice thickness monitoring, *J. Geophys. Res.*, 97(C12), 20,325-20,334, 1992.

Wadhams, P: *Ice in the Oceans, Gordon and Breach Science Publishers*, 2000.

Warren, S. G., I. G. Rigor, N. Untersteiner, V. F. Radionov, N. N. Bryazgin, Y. I. Aleksandrov, and R. Colony: Snow Depth on Arctic Sea Ice, *J. of Climate*, 12(6), 1814-1829, 1999.

Wingham, D. J.: Elevation change of the Greenland Ice Sheet, *Phil. Trans. Roy. Soc. Lond.*, 352, 1995.

Wingham, D. J., O. Johannessen, P. Lemke, C. C. Tscherning, G. Picardi, S. Sandven, D. Vaughan, S. Laxon, and R. Sharroo: CryoSat: Response to the ESA Earth Explorer Opportunity Mission AO, *University College London*, 1998.

Wingham, D. J., The First of the European Space Agency's Opportunity Missions: CryoSat, *Earth Observation Quarterly*, 63, European Space Agency, 1999.

ACRONYMS

AGMASCO	Airborne Geoid MAPPING System for Coastal Oceanography
ASAR	Advanced Synthetic Aperture Radar
ASIRAS	Airborne Synthetic aperture and Interferometric Radar Altimeter System
AWI	Alfred Wegener Institute, Germany
CRYOVEX	CRYOsat Validation EXperiment
CVRT	CryoSat Calibration and Validation Retrieval Team
D2P	Delay Doppler Phase-monopulse radar altimeter
DNSC	Danish National Space Center
DORIS	Doppler Orbit and Radio Positioning Integrated by Satellite
ECMWF	European Centre for Medium scale Weather Forecasts
EGIG	Expédition Glaciologique Internationale au Groenland
Envisat	Environmental Satellite, ESA
ERS	European Remote Sensing Satellite
ESA	European Space Agency
ESAG	European Survey of Arctic Gravity
FY	First Year (sea ice)
GPS	Global Positioning System
GreenICE	Greenland Ice and Climate Experiment
HEM	Helicopter-borne ElectroMagnetic system
IMU	Inertial Measurement Unit
INS	Inertial Navigation System
ICESat	Ice, Cloud, and Elevation Satellite
JASON	US/French ocean observation radar altimeter satellite (continuation of the TOPEX/POSEIDON mission)
JHU/APL	Johns Hopkins University/Applied Physics Laboratory, US
KMS	Kort og MatrikelStyrelsen (National Survey and Cadastre)
LaRA	Laser and Radar Altimetry campaign
LRM	Low Resolution Mode
LRR	Laser Retro-Reflector
NASA	National Aeronautics and Space Administration, US
MY	Multi-Year (sea ice)
SAR	Synthetic Aperture Radar
SARin	Synthetic Aperture Radar, interferometric (mode)
SIRAL	SAR Interferometric Radar ALtimeter
SITHOS	Sea Ice Thickness Observation Systems
SPICE	Space Borne Measurements of Arctic Glaciers and Implications for Sea Level
UCL	University College London, UK